

ERRATA

Page	Line	Read	For
59	Fig.40(B)	R^C_E	R_N
63	Line 7	of	oi
90	Line 18	Table 27	Table 28
92	Table 29, Watheroo,	$1.5 \cdot 10^3$	$15 \cdot 10^3$
99	Line 5(from the bottom)	an	on
100	Line 11	$\varphi^{0_2} = \varphi^{1_2}$	$\varphi^{0_2} - \varphi^{1_2}$
	Line 16	E^{1_2}	E^{0_2}
104	Line 15(from the bottom)	commencements	comments
	Line 4(from the bottom)	impulse	in pulse

The Local Characteristics of Earth-Currents (III)*

By TAKASABURO YOSHIMATSU

CHAPTER II

UNIVERSAL EARTH-CURRENTS AND THEIR LOCAL CHARACTERISTICS

§ 3. Time variations of the mode of Sq of earth-currents and solar activity

1. *Introduction*

In the preceding paragraph has been studied experimentally the problem of the principal direction of earth-currents observed at several stations over the world. As a next step the local characteristics of the magnitude of universal earth-currents are to be clarified by using available data as many as possible. However, before treating with this problem it is needed at first to see to what extent the magnitude of earth-currents can be variable under different conditions of the solar activity in order to make clearly the statement of the problem.

On the other hand, this is also useful not only for the investigation of the solar and terrestrial relationships from the side of earth-currents, but also for the purpose of studying any other kind of local or world-wide phenomena, not suffered from the solar influence. In this paragraph will be discussed various subjects in such a field of interest with respect to the time variations of the mode of Sq at many stations over the world, especially at Kakioka.

2. *Correlation between maximum range of Sq of earth-currents and relative sunspot number*

[A]. *Statistics for calm days*

In recent years relatively long continued observations of earth-currents have been carried out, or continuing up to date at the following four observatories, Tucson, Arizona, U. S. A.; Huancayo, Peru; Watheroo, West Australia and Kakioka, Japan.

* Continuation from the two previous papers on the same title.

L. A. Bauer⁽⁴⁾ has studied something about the solar and terrestrial relationships from the side of earth-currents observed at Ebro, Tortosa, Spain, during the interval 1914-1918. For the present investigation as a measure of the solar influence upon the potential gradient of the daily variation is simply adopted the maximum range, R , of each annual mean Sq, because it is simple and sufficient for the present purpose. By this means the relationship between R and annual sunspot number S (Zürich) was studied by using the available data at these observatories during the latest one or two sunspot cycles. At first the following three possible expressions for the correlation between R and S are examined in respect to the maximum range of east-component for all days at Kakioka in the period from 1934 to 1951,

$$R_1 = \alpha_1 + \beta_1 \cdot S, \quad R_2 = \alpha_2 + \beta_2 \cdot S + \gamma_2 \cdot S^2, \quad R_3 = a(S+b)^{1/2}.$$

The various constants contained in R 's and $\sum \left| \frac{\text{cal.} - \text{obs.}}{\text{obs.}} \right| / 18$ are calculated as follows in unit of mV/km,

	α	β	γ	a	b	$\sum \left \frac{\text{cal.} - \text{obs.}}{\text{obs.}} \right / 18$
R_1	16.6	0.0462				0.059
R_2	16.8	0.0255	$0.012 \cdot 10^{-2}$			0.054
R_3				1.37	143	0.058

where one can find no superiority of any one expression as compared with others as far as these data are concerned.

Therefore, for the sake of simplicity the linear expression given by R_1 will be used for the following statement.

The results shown in Fig. 40 are written as follows,

$$R_B^c = R_{O,B}^c + \alpha_c^B \cdot S$$

$$R_N^c = R_{O,N}^c + \alpha_c^N \cdot S,$$

where R_B^c and R_N^c are respectively the annual mean maximum ranges given in mV/km for east-component

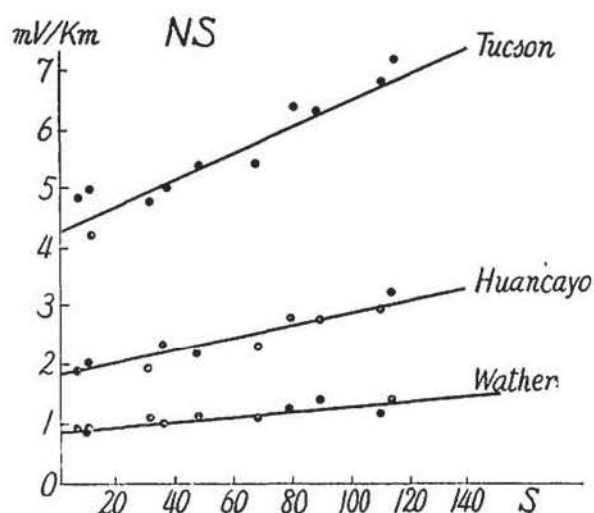


Fig. 40(A). Relationship between maximum range R_N^c of the annual mean Sq (10 least disturbed days) and relative sunspot number S , 1932-1942.

and north-component, while $R_{O,E}^c$ and $R_{O,N}^c$ are meant by fictional similar quantities which would be appeared when $S=0$. By the method of least square the coefficients α_c 's and R_0^c 's are calculated as given in Table 13(a), to which some material at Toyohara⁽⁴⁵⁾, Saghalien, is added.

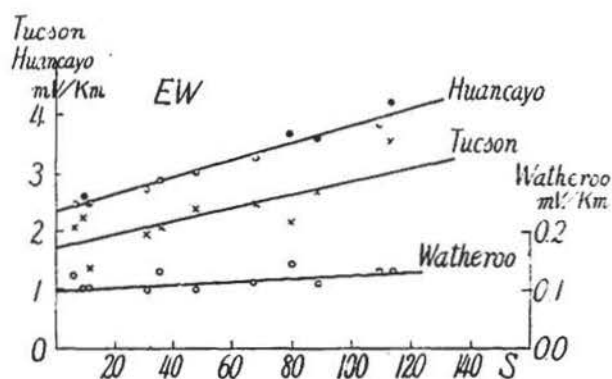


Fig. 40(B). Relationship between maximum range R_N of the annual mean Sq (10 least disturbed days) and relative sunspot number S , 1932-1942.

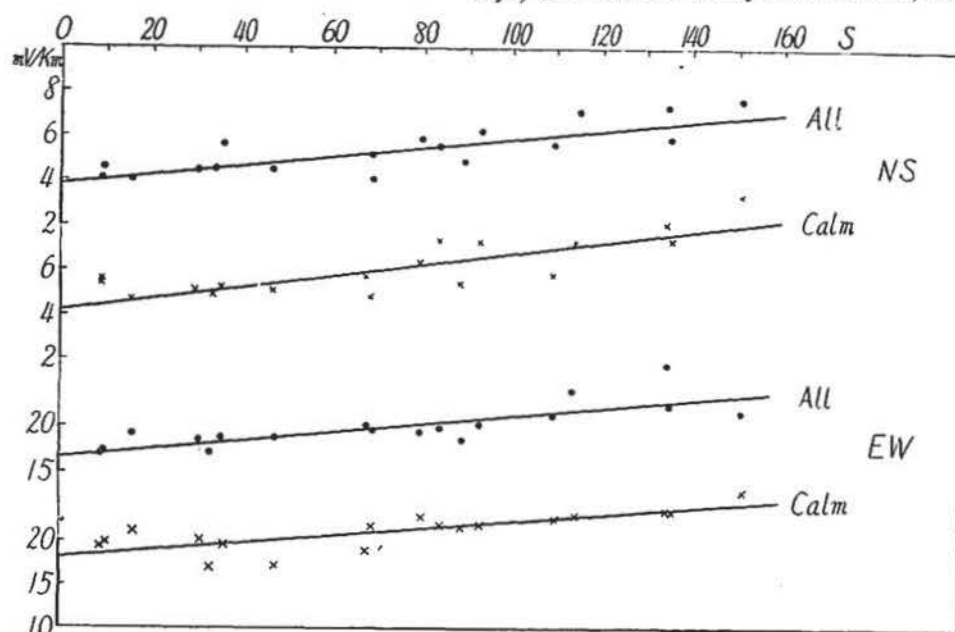


Fig. 40(C). Relationship between maximum ranges R_N and R_E of the annual mean Sq and relative sunspot number S , Kakioka.
Calm days : 1934-1945. All days : 1934-1951.

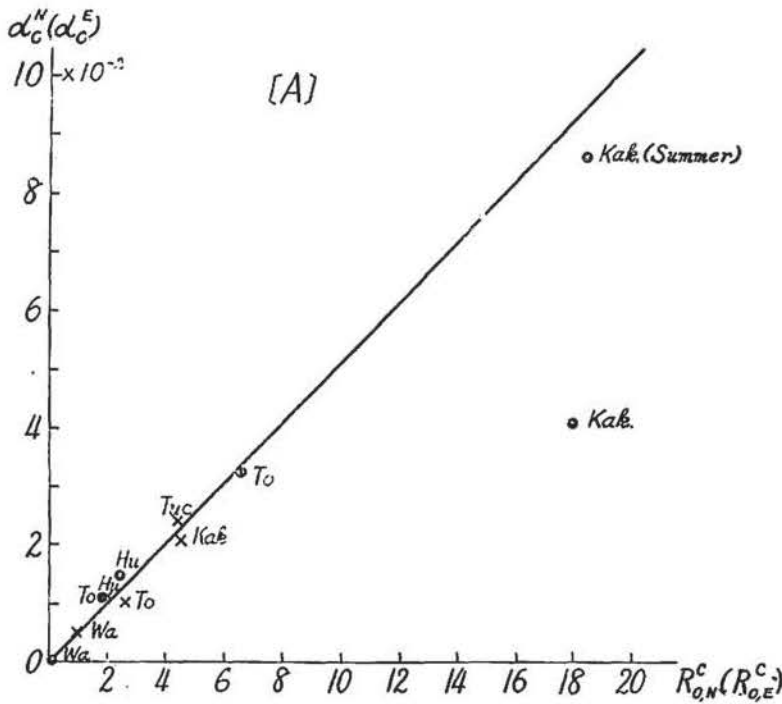
Table 13. Relationship between the maximum ranges of the annual mean Sq and relative sunspot number (Zürich).

(a) Calm days.

Station	Latitude	$R_{O,N}^c$	$R_{O,E}^c$	$100 \alpha_c^N$	$100 \alpha_c^E$	Period
Watheroo	30° 19.1 S	0.86	0.10	0.49	0.02	} 10-calm days, 1932-1942
Huancayo	12 02.7 S	1.89	2.36	1.12	1.46	
Tucson	32 14.8 N	4.37	1.75	2.36	1.10	
Kakioka	36 13.9 N	4.20	18.0	2.63	4.00	5-calm days, 1934-1951
Toyohara	46 58 N	2.60	6.60	0.99	3.23	5-calm days, 1933-1936

(b) All days.

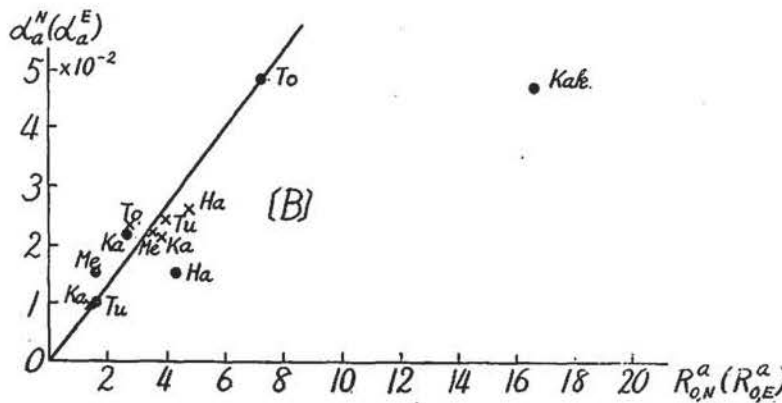
Station	Latitude	$R_{O,N}^a$	$R_{O,E}^a$	$100\alpha_a^N$	$100\alpha_a^E$	Period
Tucson	32° 14.8' N	3.99	1.62	2.39	0.99	1932—1942
Kakioka	36 13.9 N	3.84	16.6	2.09	4.26	1934—1951
Toyohara	46 58 N	2.70	7.30	2.30	4.82	1933—1936
Haranomachi	37 37 N	4.8	4.3	2.6	1.5	1947—1951
Kanoya	31 25 N	1.4	2.7	1.0	2.2	1950—1952
Memambetsu	43 55 N	3.6	1.4	2.3	1.5	1950—1953



As seen in Fig. 41(A) the connection between R_o 's and α 's manifests approximately a definite common straight line passing through the origin, not depending upon the direction of the base line. The two expressions mentioned above, therefore, can be rewritten in the following single form,

$$R_c = R_o^c (1 + m_c \cdot S),$$

$$m_c = 0.54 \cdot 10^{-2}.$$



The magnitude of m_c nearly equals to that of the similar quantity which is well-known in the fields of geomagnetism and ionosphere. The east-

Fig. 41. Relation between $\alpha^N(\alpha^E)$ and $R_{O,N}(R_{O,E})$ for calm and all days. Suffix c : Calm days, a : All days; Black circle : East-component; Cross mark : North-component.

component at Kakioka, however, deviates so much from the line that it shows no such distinct relationship, but for the summer season it holds fairly good. On this point a precise discussion will be made in later paragraphs.

On the other hand, if one looks more precisely at the distribution of points in these figures, apart from the general feature mentioned above, one notices some interesting mode of changes, for example, yearly rate of change of R_e does not seem to be constant, but slightly differs for different solar cycles, and even for components. And also during some intervals, namely, near the maximum or minimum epoch of S when the curve of S changes slowly, observed values fluctuate more remarkably than others. The latter seems to be more conspicuous at Tucson and especially so at Kakioka, and this point will be also retouched in latter paragraphs.

[B]. *Statistics for all days*

Regarding the case for all days' mean the result is given in Table 13 (b) and graphically shown in Fig. 41(B), adding the similar data at three stations in Japan; Haranomachi, Kanoya and Memambetsu, where earth-currents observations have been continued up to date for some years (Fig. 42).

The expression corresponding to R_e is given as follows,

$$R_a = R_0^a (1 + m_a \cdot S), \quad m_a = 0.54 \cdot 10^{-2},$$

where the values of east-component at both Kakioka and Haranomachi are excluded from the computation of R_a because of the same reason as mentioned above in the case for calm days. Comparing (A) statistics with (B), it is safely said that there is no appreciable difference between two solar proportional constants m_e and m_a as far as the present statistics are concerned.

[C]. *Seasonal changes of S_q of earth-currents and geomagnetic field at Kakioka*

In order to clarify the apparent dis-

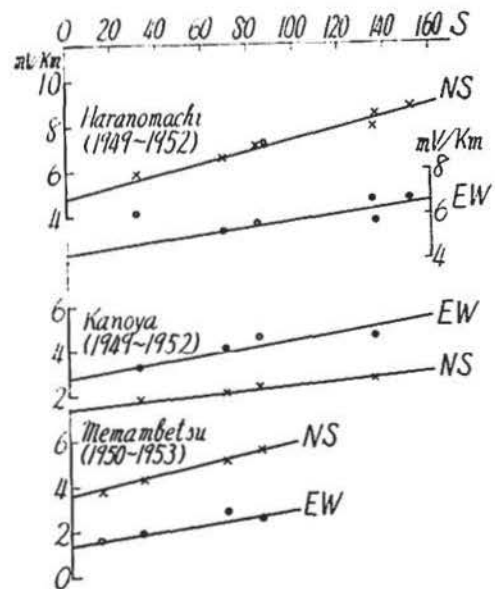


Fig. 42. Relationship between maximum ranges of the annual mean S_q for all days and relative sunspot number, Haranomachi, Kanoya and Memambetsu, Japan.

crepancy of east-component in relationship between R and S at Kakioka and in its vicinity, it is necessary to ascertain whether or not the same relation holds for each season. The maximum ranges of east component at Kakioka are given in Table 14, classifying into three seasons, equinox (III, IV, IX, X), summer (V, VI, VII, VIII,) and winter (I, II, XI, XII) for each year, 1934~1951. The calculated values of $R_{0,E}^c$ and α_c^R are given in Table 15.

From these tables one can easily accept that in the winter season R varies in wide range, and consequently α_c^R amounts merely to $1/3\sim 1/4$ times those of other seasons. Furthermore, it seems that there exists no connection between R and S in the last sunspot cycle, 1934~1944, and only appears a slight correlation in the present cycle. Contrary to these winter characteristics of the amplitude of Sq, the relation is closer in equinox, showing no definite difference between two cycles except for

Table 14. Maximum range of the solar daily variation of earth-currents for each season for east-component at Kakioka, 1934-1951. (calm days)

Year	Summer	Winter	Equinox	Year	Summer	Winter	Equinox
	mV/km	mV/km	mV/km		mV/km	mV/km	mV/km
1934	20.2	19.3	25.7	1943	19.6	15.1	31.5
35	19.7	18.7	20.2	44	26.1	18.4	21.5
36	30.4	17.5	25.6	45	18.5	19.2	16.8
37	24.9	19.4	27.6	46	20.7	21.5	22.2
38	27.4	17.6	24.6	47	31.1	22.5	27.6
39	25.6	13.8	30.4	48	32.7	22.9	26.8
40	23.8	19.9	23.4	49	30.9	27.6	27.0
41	18.4	18.4	20.5	50	25.5	23.3	25.1
42	22.9	18.9	20.6	51	27.9	21.9	24.8

Table 15. $R_{0,E}^c$ and α_c^R for each season at Kakioka, 1934-1951.

	Summer	Winter	Equinox
$R_{0,E}^c$	18.0 mV/km	18.6 mV/km	18.4 mV/km
α_c^R	$9.5 \cdot 10^{-2}$	$2.4 \cdot 10^{-2}$	$6.6 \cdot 10^{-2}$

two larger values of R 's in 1934 and 1943, these values being omitted from the computation of Table 15. In summer, however, α_c^R becomes as large as four times that of winter, and consequently it agrees fairly well

with the value expectable from the diagram ($\alpha_c^R, R_{0,E}^c$) as shown in Fig. 41(A). The

inequality of the solar effect said above can be also detectable in other terrestrial phenomena, for example, at Washington⁽¹⁶⁾ the noon value of $f_{F_2}^o$ in winter shows about 20% smaller α in the epoch 1944 ~ 1952 than that in 1935~1943 provided the linear correlation with S . It is concluded, there-

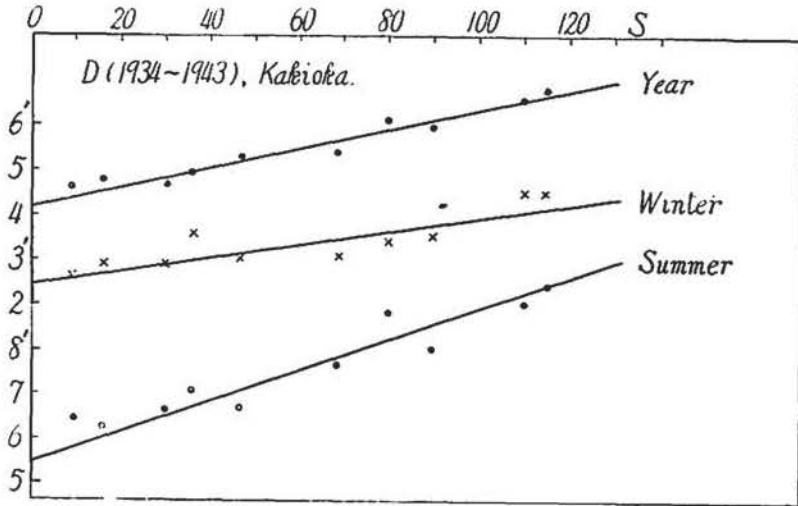


Fig. 43(A). Relationship between maximum range of geomagnetic Sq for calm days at Kakioka and relative sunspot number. (A) : Declination. (B) : Horizontal intensity.

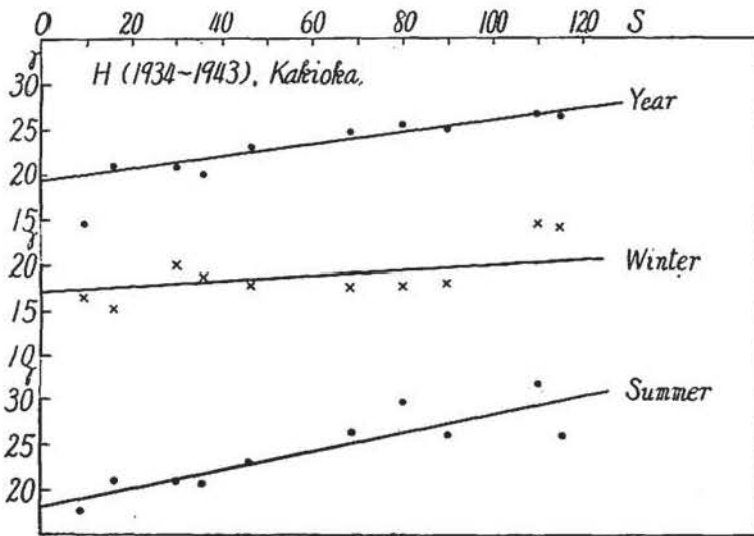


Fig. 43 (B).

fore, that Sq at Kakioka makes a remarkable seasonal change in respect to east-component, and consequently one may prefer summer to the other seasons for some investigations of the solar and terrestrial relationships in the vicinity of Kakioka.

Further, in order to support the statement

before-mentioned a similar correlation between S and the maximum range of the geomagnetic Sq-field was examined at Kakioka.

As seen easily from Table 16 and Table 17, or Fig. 43, there is scarcely a linear correlation between S and R_H^c , maximum range of Sq of the geomagnetic horizontal intensity in winter season, while a fairly good connection can be seen between S and R_D^c , maximum range for declination. The former just corresponds to the case of east-

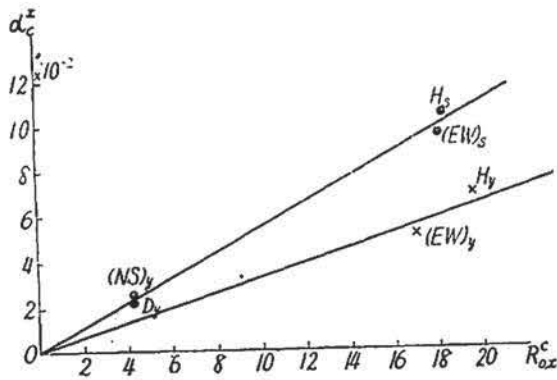


Fig. 44. Relation between α_c^x and $R_{O,x}^c$ for geomagnetic and earth-current Sq variations.

Suffix x : H, D, East-and North-component, respectively.

y : Mean for year

s : Mean for summer

component of earth-currents, while the latter does to that of north-component.

And it is also to be noted that in summer the horizontal intensity shows the closest correlation with S as east-component of earth-currents does. In Fig. 44 is shown such a correspondence between earth-currents and geomagnetic field with respect to α_c^x 's, where suffix x represents H, D, Z, E and N, respectively.

This intimate connection between earth-currents and geomagnetic field

obtained here confirms that an abnormally small amplitude of east-component of Sq at Kakioka or in its vicinity is not caused by any extraneous effect depending on observational conditions, but does link into more significant geophysical circumstances in the region considered.

Table 16. Maximum range of the solar daily variation of geomagnetic elements at Kakioka, 1934-1943 (calm days).

Year	Summer			Winter			Year		
	H	D	Z	H	D	Z	H	D	Z
1934	17.6 ^γ	6.47 ^γ	23.1 ^γ	16.6 ^γ	2.66 ^γ	11.5 ^γ	14.5 ^γ	4.60 ^γ	17.1 ^γ
35	20.6	7.02	27.6	18.8	3.60	15.0	20.1	4.89	20.0
36	29.9	8.81	31.9	17.7	3.40	20.3	25.5	6.11	26.7
37	25.8	9.44	33.4	24.3	4.49	25.0	26.6	6.80	28.8
38	32.2	9.01	30.8	24.7	4.48	21.8	26.9	6.56	25.7
39	26.2	8.03	28.3	18.1	3.53	17.8	25.1	5.95	23.4
40	26.4	7.70	22.9	17.7	3.09	17.3	24.8	5.39	21.0
41	23.0	6.70	21.2	17.9	3.01	16.4	23.1	5.29	18.3
42	21.0	6.67	20.7	20.1	2.90	16.8	20.8	4.64	19.1
43	21.1	6.25	18.6	15.0	2.92	13.4	21.1	4.76	17.0

Table 17. $R_{0,x}^c$ and α_c^x for the geomagnetic three elements at Kakioka ($x : H, D, Z$).

	Summer			Winter			Year		
	H	D	Z	H	D	Z	H	D	Z
$R_{0,x}^c$	17.5 ^γ	5.5 [']	18.7 ^γ	17.3 ^γ	2.5 [']	11.7 ^γ	19.5 ^γ	4.2 [']	14.6 ^γ
100 α_c^x	11.2	3.4	11.3	2.7	1.4	9.3	6.9	2.2	11.5

3. Long period change of the mode of Sq in winter at Kakioka and sunspot number

[A]. Introduction

In connection with the phenomena of abnormally decreasing amplitude of east-component of earth-currents at Kakioka, it seems to be important to touch further some characteristic changes of the mode of Sq in the course of long years.

Kakioka may be probably a typical station in the middle latitude encountering with different mode of distribution of the northern focus of the equivalent overhead current system of Sq. And it has been recently established⁽⁴⁷⁾ by using the data of the Second Polar Year that the intensity and position of foci of Sq frequently make remarkable changes. The matter, however, has been scarcely known yet about how does this mode change in the long course of time, especially with respect to the solar activity. Although the following statistics are mainly based on the data at Kakioka during the latest two sunspot cycles, they may contribute a new information to the question stated above.

[B]. Long period change of T_{min}^R , time of occurrence of the extreme minimum of Sq of earth-currents, in winter at Kakioka

The form of Sq at Kakioka is such as shown in Fig. 45, in which positive sense is used when the current flows eastwards or northwards. It should be, however, emphasized that the form of Sq shown in the figure, that is, the mode of occurrence

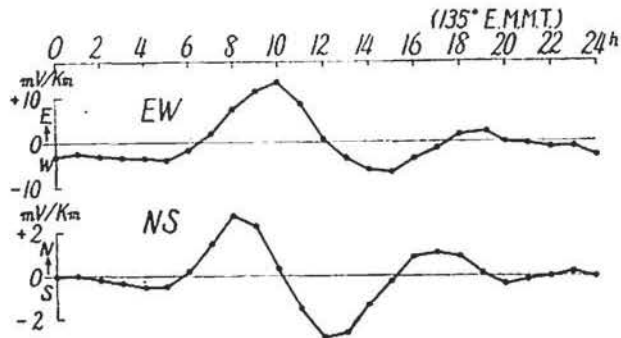


Fig. 45. Yearly mean Sq of earth-current potential gradient at Kakioka, 1934~1944 (five calm days).

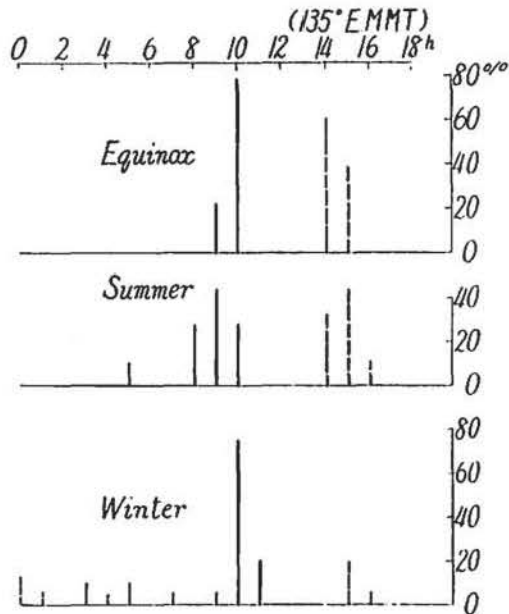


Fig. 46. Hourly frequencies of occurrence of extreme maximum and minimum of Sq for east-component, 1934-1951, (calm days).
Solid line : extreme maximum.
Broken line : extreme minimum.

winter, therefore, the extreme minimum of Sq appears for the most time in early morning, contrary to the mode of Sq in summer or equinox. The time variations of T_{max}^E and T_{min}^E for each annual mean Sq are shown in Fig. 47, denoting by the marks max. and min., respectively. It is clearly seen in the figure that out of total twenty years only five years show the extreme minimum of Sq in the afternoon. Furthermore, it should be noticed that all these five years are situated in the increasing phases of sunspot numbers as far as the latest two sunspot cycles are concerned. As a whole, T_{min}^E undergoes a remarkable long period change with the maximum about two years before the maximum year of S, but the form of the curve is dissimilar with that of S itself. Concerning this point, however, it was found out that there is a good parallelism between the curve and that of $\Delta S/\Delta t = S_{n+1} - S_n$, successive difference of annual sunspot numbers, which are plotted for the middle of two consecutive years. In other words, it is found out that even in winter there exists an intimate connection between R and S, if such a new measure is taken into consideration for the inequality of the form of Sq.

At last it may be worthy to touch again the problem of T_{min}^E in winter in an

of the extreme values does not remain constant in the course of the sunspot cycle.

For the first time a remarkable difference between winter and the other two seasons can be seen in the hourly frequency distribution of T_{min}^E , as shown in Fig. 46. This seasonal inequality is most conspicuous for east-component in winter.

Concerning T_{max}^E , occurrence time of the extreme maximum, one can find no such a thing. Then, in the following statement one may confine himself to T_{min}^E of east-component in winter only. The frequency of occurrence of T_{min}^E in the forenoon hours amounts to 75% of the total number during the period 1934~1951. In

another way. Let the number of months satisfying $T_{min}^E > T_{max}^E$ out of four winter months be denoted by n , and its year-to-year change is examined. In Fig. 48(A) is shown the yearly change of n for east-component, manifesting a similar long period change as seen already in Fig. 47. Of course, we have a similar change for north-component, though n is larger but less amplitude of variation than east-component.

The smoothed solid curves in the figures are drawn by using four years' running average of n .

[C]. Long period change of the mode of geomagnetic Sq at Kakioka

In order to ascertain the result obtained above in another interval of years, geomagnetic Sq at Kakioka will be examined for the period 1925~1945.

Horizontal intensity H: The hourly frequency of T_{min}^H and T_{max}^H are shown in Fig. 49. The distribution of T_{min}^H is almost steady in each season within a limit of two hours of fluctuations, though there is a slight tendency in winter to occur within a few hours before the midnight. On the contrary to this, the monthly mean extreme maximum occurs during 6~9 hours by 38% of the total months in winter. In harmony with the case of earth-currents, the number of months satisfying $T_{max}^H > T_{min}^H$ out of four winter months is denoted by n , and its yearly change is shown by H_{max} in Fig. 50. The smoothed curve shows two maxima, a predominant maximum in 1927

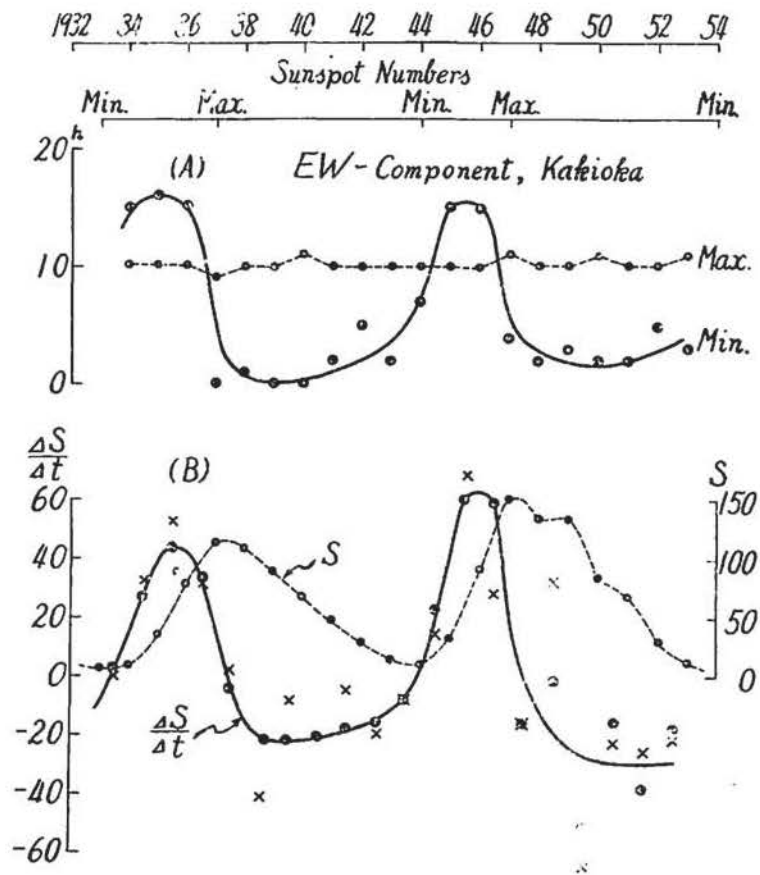


Fig. 47. Long period change of T_{min}^H of Sq for east-component in winter at Kakioka (A) and time gradient of relative sunspot number $\Delta S/\Delta t$, where Δt is one year (B). $\Delta S/\Delta t$'s for annual and winter means of S are expressed by black circles and cross marks, respectively.

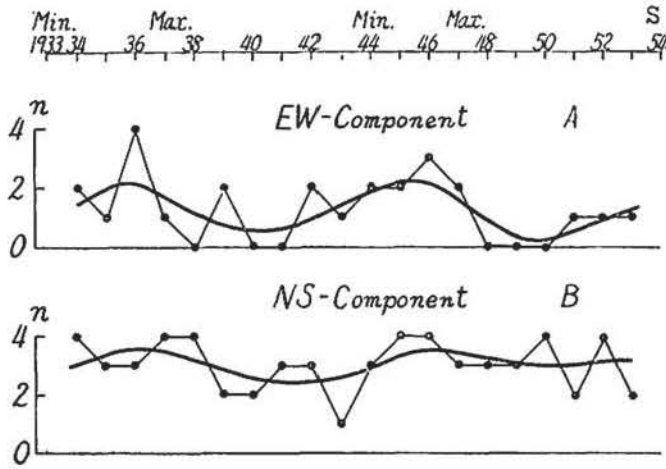


Fig. 48. Long period change of n , namely, number of months satisfying $T_{min}^E > T_{max}^E$, out of four winter months for each year at Kakioka (calm days).

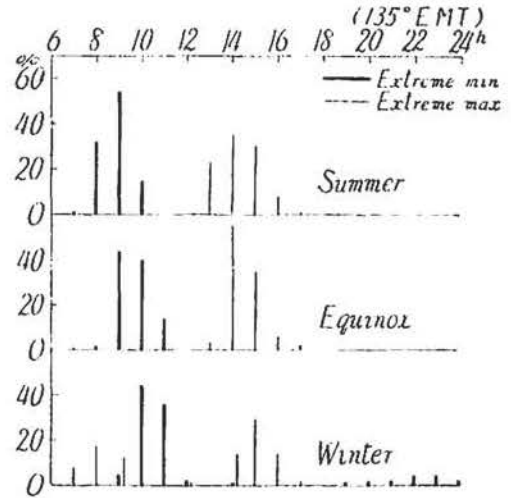


Fig. 49. Hourly frequencies of extreme maximum and minimum of geomagnetic Sq for the horizontal intensity H at Kakioka. 1925~1945 (calm days).

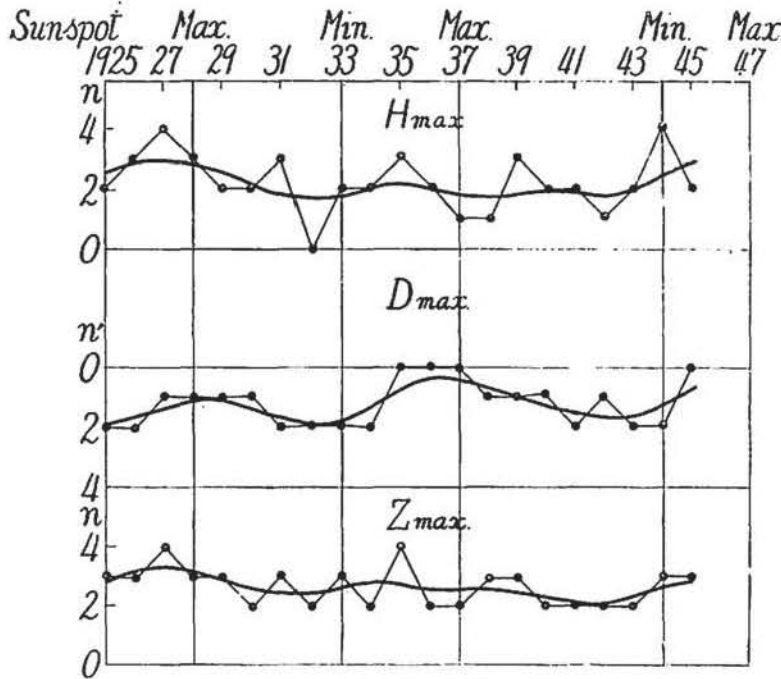


Fig. 50. Long period changes of the mode of geomagnetic Sq in winter for the horizontal intensity H , declination D and vertical intensity Z at Kakioka.

such as given in Table 18. If the number of months in winter, of which daily maxima occur earlier or later than 13hr, the most frequent time of occurrence, be denoted by n' , the year-to-year variation of n' is of a similar curve with H_{max} . as shown by D_{max} .

and less one in 1935; each occurs one or two years earlier than the maxima of S . This general tendency is in harmony pretty well with that of earth-currents.

Declination D :

Comparing with H , the form of Sq of D is remarkably stable, and the maximum and minimum occur almost at 13hr and 9hr, respectively. The frequencies of T_{max}^D , and T_{min}^D are

in Fig. 50. But the sense of variation is such that the more frequently H shows the summer-or equinox-type, the more nearly T_{max}^D approaches to 13 hr. In other words, deviations of T_{max}^D from the most frequent value, 13 hr, seem to be controlled by the same agency as governing the fluctuations of T_{max}^H .

Table 18. Frequency (%) of T_{max}^D and T_{min}^D at Kakioka, 1925-1945.

	8	9	10	11	12	13	14 ^h
T_{max}^D	—	—	—	—	15	69	15
T_{min}^D	12	77	11	—	—	—	—

Vertical intensity Z: T_{min}^Z appears in the interval 8 hr~11 hr, namely, 50% at 9 hr, and 83% in 9 hr~10 hr, while T_{max}^Z appears in two groups of hours, 4 hr~8 hr and 13 hr~16 hr, respectively. The time variation of n , which is calculated for the afternoon maximum, is given by the lowest curve in Fig. 50, showing a similar tendency with the other two magnetic elements.

[D]. Relationship between n and frequency of so-called "E-type" of Sq in winter at Kakioka

At last the variation of n of any element said above, say, east-component of earth-currents is directly compared with that of frequency of "E-type" of Sq in winter, N , the result being shown in Fig. 51 during the latest sunspot cycle, 1944~1953. It is natural to find a good parallelism between two curves, because characteristics

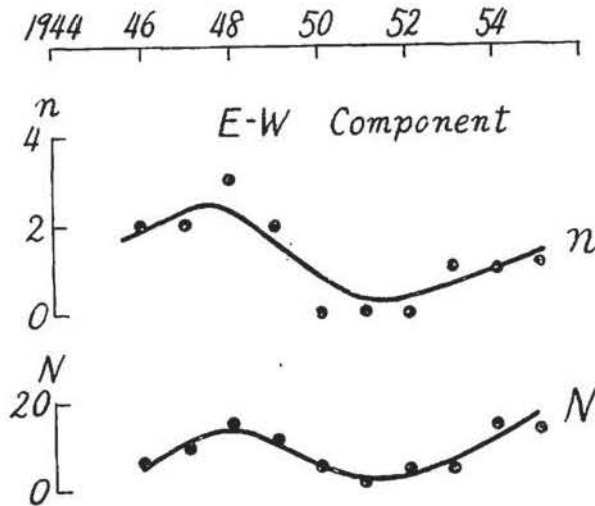


Fig. 51. Long period variations of n and N in winter at Kakioka.

of n ought to be controlled by N . The criterion for classifying the type of the solar daily variation has been discussed by the Ionosphere Research Committee, Science Council of Japan, to which larger parts of the present data of "E-type" have been presented by the Kakioka Magnetic Observatory. Now, considering the connection between n and $\Delta S/\Delta t$ obtained above, the frequency N of "E-type" of Sq should

also be understood in the sense of $\Delta S/\Delta t$, but not S itself. On the other hand, as to the average state of Sq, the position of focus in the northern hemisphere attains its most northern latitude in the forenoon with respect to G. M. T. ^[48], while the intensity of focus in the southern hemisphere raises nearly to the maximum value. Hence, even at a station far remote from the focus, "E-type" variations may manifest themselves when the northward wandering motion of foci is strengthened. The variation of N at Kakioka, therefore, seems to be apparently due to the remarkably intensified ionization, or enlarged integrated conductivity, of the ionosphere in the southern hemisphere. But, from ionospheric observational results and others, the yearly change of ionization of the ionosphere, or magnitude of integrated conductivity, seems to depend solely upon S itself, but not $\Delta S/\Delta t$. Hence, it may be apparently suggested that if the sun does not emit some special kinds of short waves during the rapidly raising interval of S , namely one or two years before the maximum of S , the ionospheric motion would be subjected by some unknown mechanism in the ionosphere to intensify the equivalent current system with the same long period as n or N . Nevertheless, at present one has no sufficient observations such as to be able to check possible considerations said above.

At any rate, however, these facts obtained in the vicinity of variable locus of foci of Sq may throw a light on the theory of Sq, especially its secular change. At the same time some predictable informations of the type of Sq will become useful for some practical geomagnetic and geoelectric workers.

[E]. *Long period change of the mode of Sq of earth-currents in winter at Tucson*

A similar treatment with Sq was carried out for another middle latitude station, Tucson, Arizona, U. S. A. ^[49], of which material covers the former sunspot cycle 1932 ~1944, but not long enough for the present object. The seasonal variation of earth-current potential gradients at Tucson has been already discussed by W. J. Rooney ^[50], while the present treatment is confined itself to the behavior of Sq in winter months only in comparison with the result at Kakioka. The form of the solar daily variation at Tucson is such as shown in Fig. 52.

In Table 19 are given the average values of T_{max}^H and T_{min}^H , for each month as well as the frequency of deviations from the corresponding average values. The average

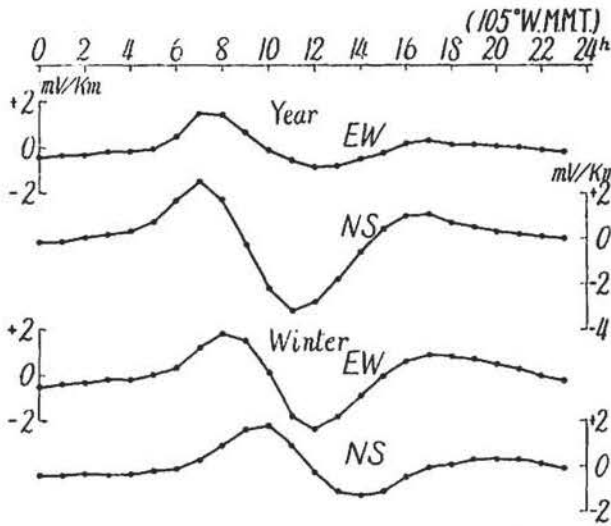


Fig. 52. Sq for 10 least disturbed days per month at Tucson, 1932~1942.

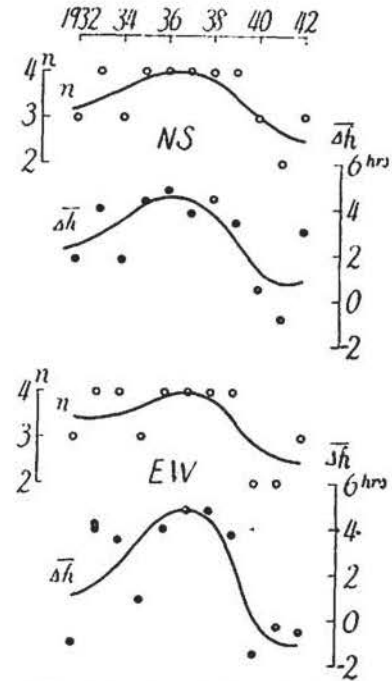


Fig. 53. Long period changes of n and Δh at Tucson.

values of T_{max}^E and T_{min}^E are nearly constant for each month in respect to the whole period as well as an individual year.

The number of months n , in which average time of occurrence of the extreme

Table 19. Frequencies of time of occurrence of the extreme values of S_q in winter at Tucson, 10 least disturbed days, 1932~1942.

Component	Average time of occurrence of the extreme values for each month. (1)			Number of months corresponding to the following deviations of hours from (1).													
	Extreme value	Month	Average time (hr)	-14	-12	-3	-2	-1	0	1	2	6	7	8	9	10	11
NS	min.	I	12 ~ 13						1	8	2						
		II	12 ~ 13						1	9	1						
		XI	12 ~ 13		1				3	6			1				
		XII	12 ~ 13							8	3						
NS	max.	I	9 ~ 10						3	8							
		II	8 ~ 9						2	5	1			2	1		
		XI	7 ~ 8							8	2	1					
		XII	9 ~ 10						5	4				2			
EW	min.	I	14 ~ 15						1	9	1						
		II	14 ~ 15		2	2			3	2							
		XI	15 ~ 16		1		3	2		5							
		XII	15 ~ 16		2	2		1	3	2	1						
EW	max.	I	10 ~ 11						1	9	1						1
		II	9 ~ 10						2	1	2	3		1			
		XI	8 ~ 9			1			3	5	2						
		XII	10 ~ 11						3	5	3						

minimum lags behind that of the extreme maximum, is distributed as shown in Fig. 53, where $n \geq 2$ for both components. In the figure is also shown a quantity Δh , which is the average value of $\Delta h = T_{min}^E - T_{max}^E$. Comparing these results with those at Kakioka, a similar tendency can be found, but less remarkable at Tucson. This is probably due to the inequality of their relative positions to the focus of the Sq current system in spite of their nearly same geographical coordinate of latitude.

4. 4-year period change of the mode of Sq in winter at Kakioka

(A). Shorter periodic changes of n of earth-currents and geomagnetic field

Following the preceding paragraph a further detailed analysis of the time variation of the occurrence time of the extreme values will be performed in this paragraph.

It is easily found out in Fig. 48 or Fig. 50 that there may exist some shorter periodic variations superposed on the long period change mentioned above. Since apparently fluctuations with about 4-year period can be seen in these figures, the

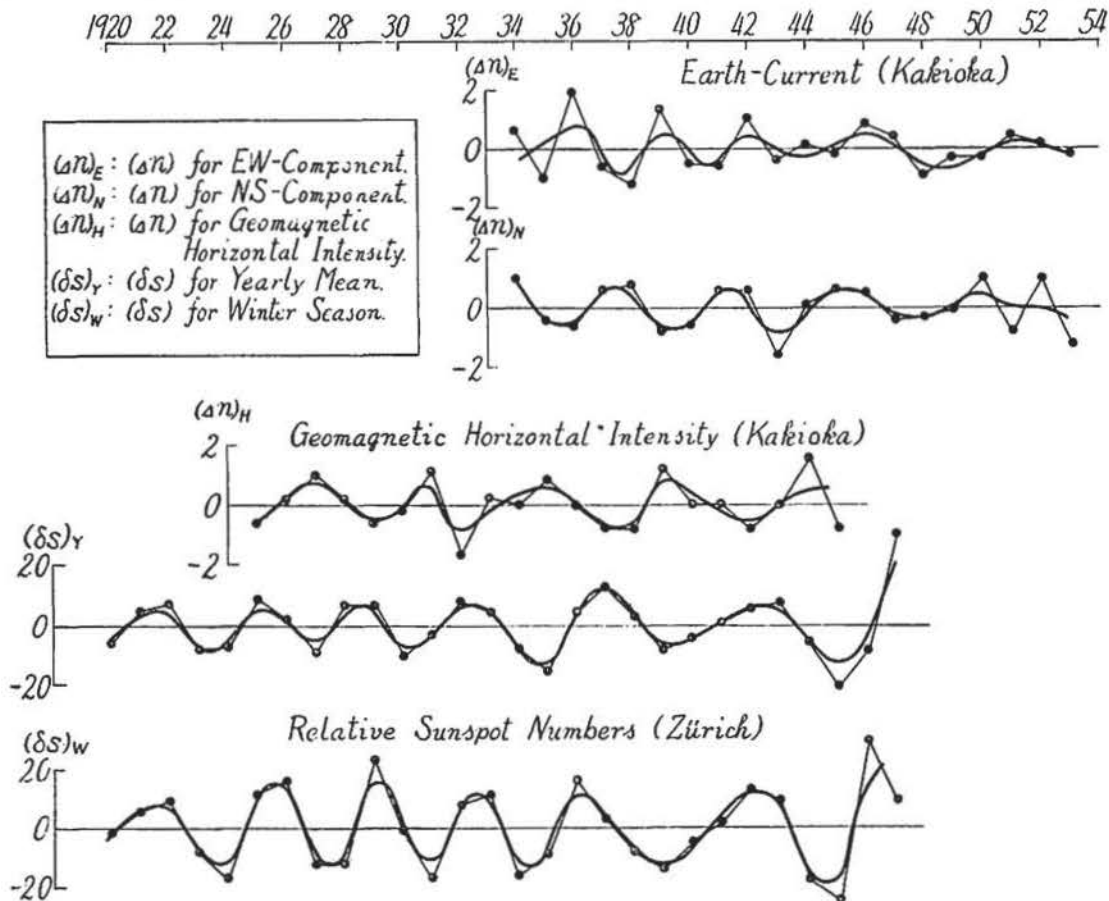


Fig. 54. 4-year period change of the mode of Sq in winter at Kakioka and its connection with that of S .

residuals $(\Delta n)_x = n_x - \bar{n}_x$ are calculated for the convenience of the study of shorter periodic changes, where the suffix x is to be read as N , E and H for north-component, east-component of earth-currents and geomagnetic horizontal intensity, respectively, \bar{n}_x being the 4 years' running average of n . They are shown in Fig. 54.

$(\Delta n)_N$: During the interval from 1934 to 1949 4-year period is apparent, while in the period 1951~1953 observational points are more or less scattered and tend to show longer period as well as increasing amplitude. At least, 4-year period in the interval 1934~1949 is statistically significant by 1.3% level of the criterion of the periodogram analysis.

$(\Delta n)_E$: In the interval 1934~1940, 3-or 4-year period are seen, and generally in an opposite sense of variation against $(\Delta n)_N$.

$(\Delta n)_H$: 4-year period is apparent, and in later years the period seems to grow longer. The variation is approximately in opposite sense against $(\Delta n)_N$.

Referring to the geomagnetic vertical intensity Z , $(\Delta n)_Z$ shows no distinct periodicity because of small amplitude.

From these facts it is evident that there is contained a predominant periodic change with period about 4 years in the time variation of Δn for both earth-current and geomagnetic field during the recent thirty years.

[B]. Δn , $f_{F_2}^\circ$ and S

It is interesting to know whether or not such a periodic change stated above does exist in the time variations of annual relative sunspot numbers S . The lowest two curves of δS in Fig. 54 will answer to this question. In order to eliminate 11-year period five years' running average of S is subtracted from S . But for convenience of treatment of data, the same process of average is repeated twice more. The final residual δS

is calculated for two cases, $(\delta S)_r$ for annual mean and $(\delta S)_w$ for winter, respectively. The connection between δS and Δn , say, $(\Delta n)_H$ is shown in Fig. 55 of which all points

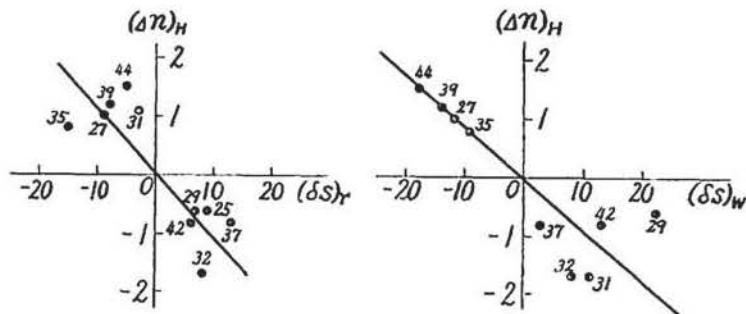


Fig. 55. Values of $(\Delta n)_H$ at Kakioka corresponding to maxima and minima of δS .

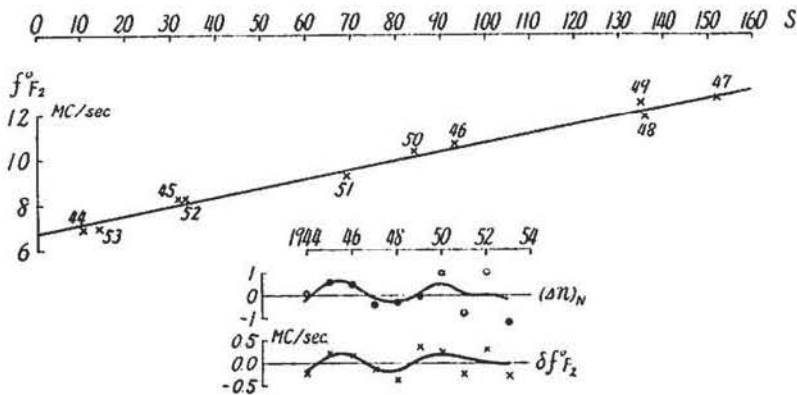


Fig. 56. Correlation between S and $f^{\circ}F_2$ in winter at Kokubunji, Japan.

correspond to the maxima and minima of δS .

There is seen clearly an inverse sense of variation between two quantities, though the numerical values do not always show so good connection, which is inevitable in such a case of treatment.

On the other hand

it is also interesting to see whether or not the corresponding shorter periodic change does exist in the time variations of the ionospheric elements. For example, in Fig. 56 are shown the correlation between $f^{\circ}F_2$ at Kokubunji, Tokyo⁽¹¹⁾ and S , together with that between $(\Delta n)_N$ and $\delta f^{\circ}F_2$. Here, $f^{\circ}F_2$ is the average noon value for each winter, and $\delta f^{\circ}F_2$ the deviation of $f^{\circ}F_2$ from a linear expression $f^{\circ}F_2 = 6.7 - 0.041 \cdot S$ which is calculated by the method of least square. As seen in the figure a fairly good positive correlation can be found between $(\Delta n)_N$ and $\delta f^{\circ}F_2$, showing that the ionosphere over Kokubunji in winter may be simultaneously changeable in a similar way as Sq field, since Sq is mainly originated in the E -layer. A similar change of $\delta f^{\circ}F_2$ can be more or less found at Washington⁽⁶²⁾ and other middle latitude ionospheric stations.

At last it may be worthy to add some remarks that if the calculation of $(\delta S)_Y$ is extended to the former century, almost all large peaks of the maximum values of $(\delta S)_Y$ fall on the respective sunspot maximum years (Table 20). Moreover, it is likely that $(\delta S)_Y$ contains some longer periods, say, two or four times the

Table 20. Maximum values of $(\delta S)_Y$.

Year	$(\delta S)_Y$	Year	$(\delta S)_Y$	Year	$(\delta S)_Y$
1832	11	1974	3	1909	7
36	31	77	12	12	8
41	4	81	10	17	21
45	3	84	7	22	7
48	25	89	5	25	9
52	8	92	13	28	8
54	1	98	1	32	13
59	15	1900	7	37	8
64	11	5	8	43	31
70	30				

primary sunspot period, 11 years.

5. Harmonic analysis of Sq of earth-currents

[A]. Harmonic analysis of Sq of earth-currents at Kakioka

The results of harmonic analysis of Sq up to the fourth harmonics are given in Table 21 for each year^[53]. Fourier terms are expressed by $E(N) = \sum_n C_n \sin(nT + \varphi_n)$, where φ_n is measured from the midnight of the universal time T .

In the first place, the correlation between C_n^a for all days and S can be approximately expressed as follows from Table 22 and Fig. 75,

$$C_n^a = C_{n,0}^a + \beta_n^a \cdot S = C_{n,0}^a (1 + m_a' \cdot S), \quad m_a' = 0.38 \cdot 10^{-2},$$

where the fourth term is excluded from the calculation because of small amplitude.

The value of m_a' is nearly equal to 0.34×10^{-2} calculated from Fig. 44 for yearly maximum range, and also to 0.42×10^{-2} , mean value for east- and north- component

Fig. 57. Relationship between β_n^a and $C_{n,0}^a$ of Sq at Kakioka, 1934~1944. Black circle : East-component. Cross mark : North-component.

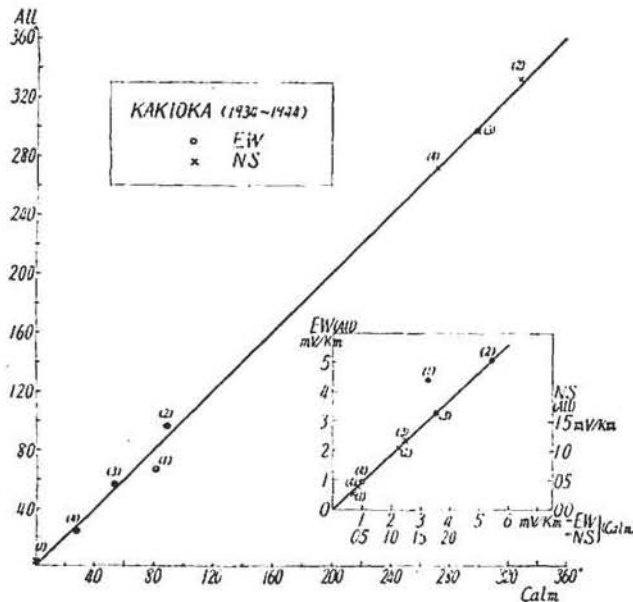
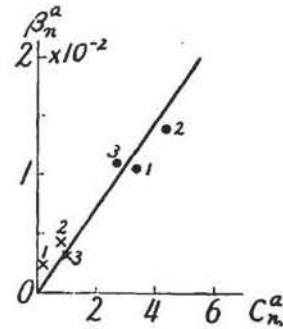


Fig. 58. Comparison of Fourier coefficients of Sq for all days and calm days at Kakioka, 1934~1944.

in Table 13.

The comparison of Fourier terms for all days with those for calm days is graphically shown in Fig. 58 for the average value in the interval 1934~1944. As seen from the figure, there is no appreciable difference between them except for the diurnal wave of east-component, though for each individual year the matter does not always hold good so because of some accidental irregularities. The amplitude of the diurnal wave of east-component is

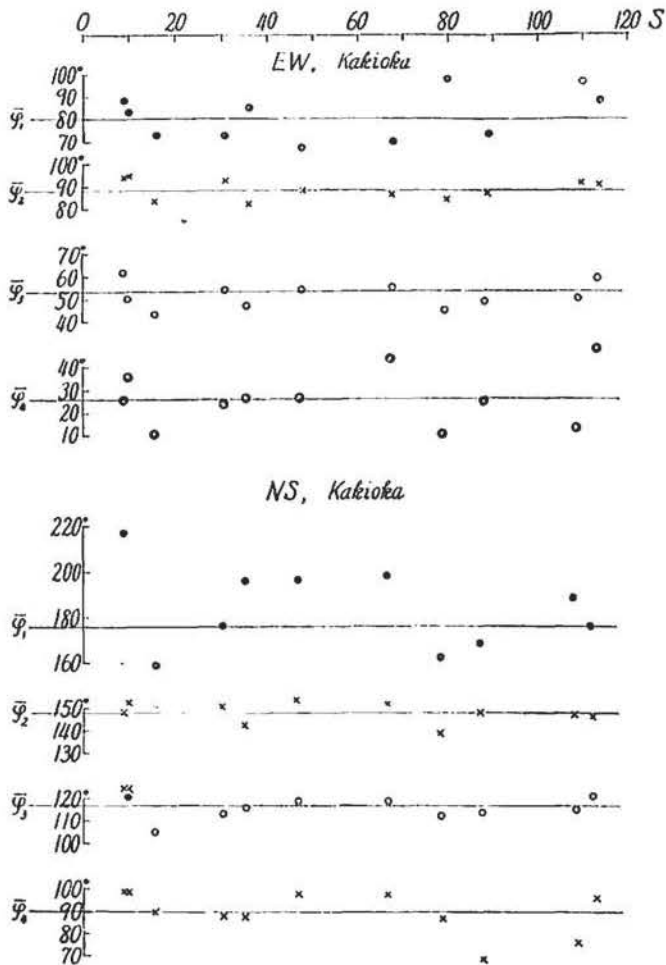


Fig. 59. Relation between phase angle φ_n of Sq for calm days at Kakioka and S , 1934~1944.

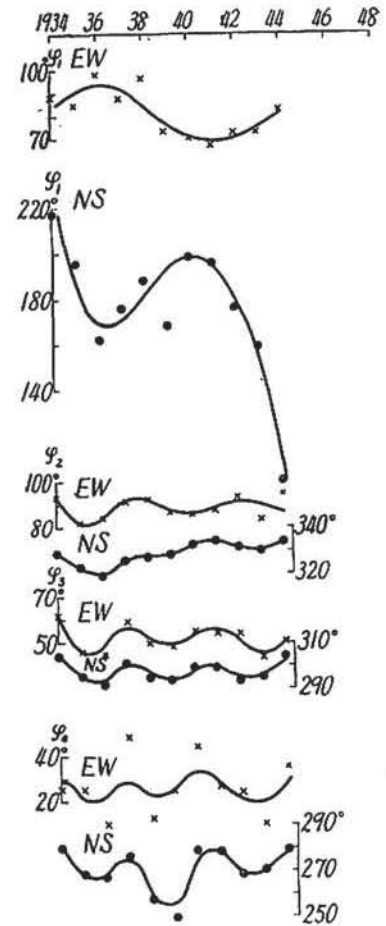


Fig. 60. Year-to-year change of φ_n of Sq for calm days at Kakioka, 1934~1944.

relatively larger for all days, while the phase angle shows only a minor difference.

Referring to this point, it may be worthy to raise a question that whether or not the solar flare effects would be intensified during prevailing disturbances as compared with those on calm days. From the result obtained here it seems to be no appreciable difference as a whole between two cases, and if any, it may be probably responsible for a contribution from the diurnal term.

In the second place, the correlation between phase angles for calm days and S is graphically shown in Fig. 59, in which $\bar{\varphi}_n$ represents the mean value for the n -th harmonic wave. It is easily seen that there is no appreciable connection between S and the phase angles of the second and third harmonic waves, the former being the largest wave of Sq. The values of φ_1 manifest apparently random large

fluctuations especially in north-component, and as a whole, there is no definite correlation between φ_1 and S .

Table 21. Fourier coefficients of Sq of earth-currents at Kakioka, 1934-1944.

$$E(N) = \sum_n C_n \sin(nT + \varphi_n). \text{ Unit : 0.01 mV/km and degree.}$$

c : Five calm days ; a : All days. + : Higher potential electrode.

Year	EW+				NS+				EW+				NS+				
	C ₁	C ₂	C ₃	C ₄	C ₁	C ₂	C ₃	C ₄	φ_1	φ_2	φ_3	φ_4	φ_1	φ_2	φ_3	φ_4	
1934	c	308	545	299	78	34	155	128	39	89	84	62	26	217	149	124	99
	a	388	480	254	59	21	97	112	34	74	95	57	30	262	154	123	93
35	c	311	515	291	66	28	101	118	34	85	82	47	26	196	143	116	88
	a	416	510	323	81	43	112	119	40	75	99	54	46	191	152	119	94
36	c	359	578	356	84	61	136	137	36	98	84	45	10	162	139	112	87
	a	435	514	321	98	60	126	123	35	72	93	46	9	162	141	111	78
37	c	324	586	451	125	64	151	157	60	88	91	59	48	176	146	121	96
	a	489	672	452	154	62	149	156	53	73	93	66	40	174	150	121	94
38	c	270	591	391	69	49	121	131	35	97	92	50	13	188	147	115	77
	a	462	602	347	59	31	121	127	31	74	95	50	6	195	149	118	83
39	c	325	599	404	125	30	118	125	39	73	87	48	25	168	148	114	69
	a	499	508	338	69	28	104	113	32	62	101	56	358	201	156	115	77
40	c	356	528	355	116	54	107	120	49	70	86	55	44	198	152	119	98
	a	512	499	367	89	38	100	117	40	64	88	54	44	210	151	111	99
41	c	364	415	317	37	36	102	110	42	67	88	54	27	196	154	119	98
	a	416	476	323	151	31	90	104	38	58	104	66	12	202	154	114	17
42	c	373	528	352	117	29	106	111	42	73	93	54	24	176	151	113	88
	a	398	478	322	122	25	87	106	39	63	104	60	12	201	153	116	52
43	c	287	517	332	114	14	97	108	46	73	13	43	11	159	150	105	90
	a	521	417	258	68	19	89	92	37	61	88	47	17	69	146	113	101
44	c	272	541	316	94	28	80	102	46	83	95	50	36	100	153	124	99
	a	341	494	311	89	26	80	100	44	64	104	62	33	72	165	127	98
1934~1944	c	317	539	350	97	36	113	122	41	81	89	52	27	180	148	118	91
	a	422	511	327	90	27	106	115	38	67	97	57	24	184	152	117	92

On the other hand, if year-to-year changes of φ_n are drawn in Fig. 60, there is seen a corresponding systematic change for each φ_n , but a remarkable inequality between φ_1 and others. This is ready to remind of contrast of variation between n and Δn as already mentioned. That is to say, the mode of time variation of φ_1 corresponds to that of n , while that of each other φ_n to that of

Table 22. Amplitude of Fourier coefficients at Kakioka. (mV/km)

n	$C_{n,o}^a$		$100\beta_n^a$	
	NS	EW	NS	EW
1	0.22	3.38	0.24	1.05
2	0.81	4.37	0.43	1.39
3	1.00	2.67	0.32	1.10

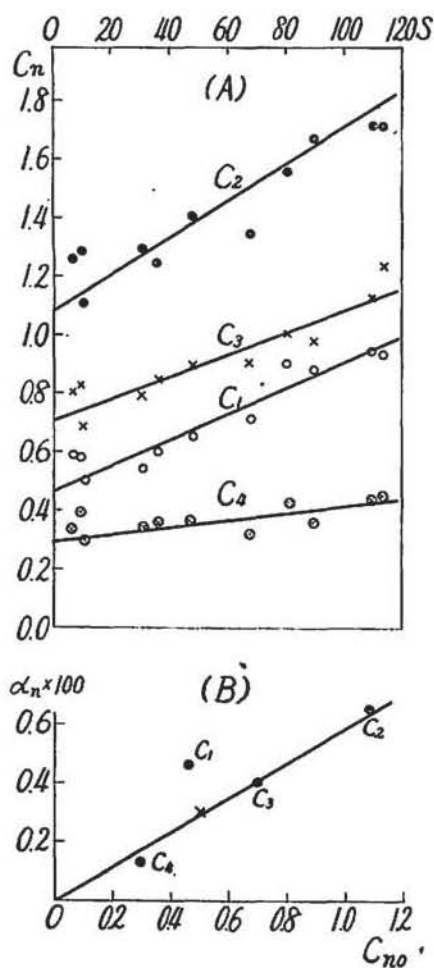


Fig. 61. Correlation between Fourier coefficients C_n 's of Sq at Tucson and S .

Δn . In other words, the periodic change with 4-year period of Δn may be primarily responsible for higher harmonic waves, but not for the diurnal one. On the contrary the long period change of n or N , which bears a striking resemblance to that of $\Delta S/\Delta t$, may be substantially responsible for the first harmonic wave.

[B]. *Harmonic analysis of Sq of earth-currents at Tucson*

For the comparison with the results at Kakioka the results of harmonic analysis of Sq deduced from 10-least disturbed days' mean at Tucson are given in Table 23 for the interval 1932~1942. The correlation between C_n and S is graphically shown in Fig. 61(A), which is of less closeness in both maximum and minimum sunspot periods as already seen at Kakioka. As a whole, however, it can be expressed as follows,

Table 23. Harmonic analysis of north-component of Sq of earth-currents at Tucson, 1932~1942 (10-least disturbed days). $N = \sum_n C_n \sin(nt + \varphi_n)$, t : 105° W. M. M. T.

		1932	1933	1934	1935	1936	1937	1938	1939	1940	1941	1942
Amplitude (mV/km)	c_1	0.50	0.59	0.58	0.60	0.90	0.94	0.95	0.88	0.71	0.65	0.54
	c_2	1.11	1.26	1.29	1.25	1.56	1.71	1.72	1.67	1.35	1.41	1.30
	c_3	0.69	0.80	0.83	0.85	1.01	1.24	1.14	0.98	0.91	0.90	0.80
	c_4	0.39	0.34	0.39	0.36	0.42	0.46	0.44	0.36	0.32	0.36	0.34
Phase (degree)	φ_1	93	82	80	74	75	68	75	73	86	89	92
	φ_2	278	276	275	274	273	272	270	270	275	279	279
	φ_3	121	118	120	116	119	117	116	118	120	127	125
	φ_4	336	333	331	330	352	338	344	342	338	347	343

$$C_n = C_{n,0} + \alpha_n \cdot S \equiv C_{n,0}(1 + m' \cdot S), \quad m' = 0.58 \cdot 10^{-2},$$

where the diurnal term is omitted from the calculation because of large deviation from this expression. This large deviation is responsible for the maximum period of S , 1936~1939, and if the values of these years are excluded from the calculation of the mean value, C_1 falls just on the line as shown by a cross mark in Fig. 61 (B); there might be something to intensify the diurnal term in this period. The value $m' = 0.58 \cdot 10^{-2}$ is nearly equal to $m_c = 0.54 \cdot 10^{-2}$ deduced from the (R, S) correlation, and can be reasonably expected because φ_n does not change remarkably throughout the period except for the diurnal wave.

As compared with the time variations of phase angles at Kakioka, φ_n at Tucson shows a remarkable difference in the following point (Fig. 62). The matter is that there appears no shorter periodic change, 4-year change, in each phase angle at Tucson, keeping a nearly constant respective value each other throughout the period except for φ_1 , which shows a similar long period change at both stations as already

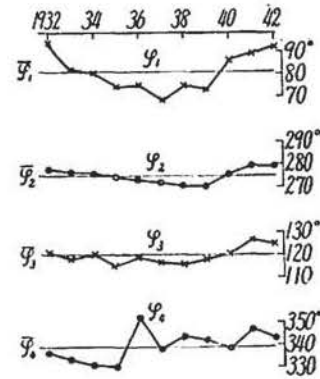


Fig. 62. Year-to-year changes of phase angles φ_n 's of Sq at Tucson.

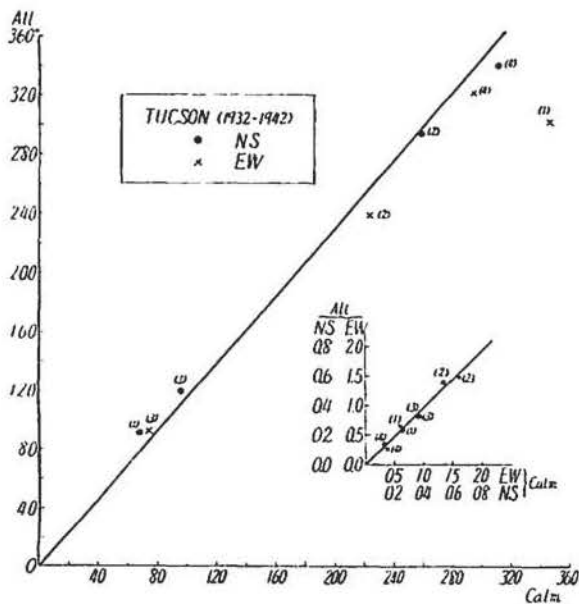


Fig 63. Comparison of Fourier coefficients of Sq for all days' mean and calm days' one at Tucson, 1932~1942.

mentioned. It seems likely that the ionosphere over Tucson exerts a different kind of action upon the mode of year-to-year change of Sq as compared with that over Kakioka. Regarding this discrepancy between two observatories, it may be somewhat worthy to note that the yearly rate of time variation $\delta f^{\circ} F_2$ is remarkably larger in winter at Kokubunji, while there is no appreciable difference between winter and annual means at Washington. It is desired to examine this inter-

esting behavior of the secular change of Sq field by using as many data at stations in similar situations as possible. From the same point of view, further continued observations of earth-currents at Tucson, if possible, will play an important role for clarification of these long period changes of Sq and other transient phenomena, some of which may be responsible for some multiple or higher harmonics of 11-year period of sunspot numbers.

The comparison of Sq for calm days' mean with that for all days' mean is graphically shown in Fig. 63, in which no appreciable difference can be seen between them except for φ_1 .

§ 4. Magnitude of earth-current potential gradient and its local characteristics

1. World-wide data of Sq referred to some solar activity state

The results of harmonic analysis of potential gradient of Sq observed at various stations over the world are given in Table 24, where north- and east-component are expressed as follows,

$$N = \sum_n C_n^N \sin (nt + \alpha_n), \quad E = \sum_n C_n^E \sin (nt + \beta_n),$$

and t is measured from midnight of the local standard time, positive direction being reckoned towards east and north. These data, however, are based on various kinds of sources, that is, different interval of observations, different epoch of the solar activity, different character of adopted days and so forth. So, they are not suitable for the synthetic study of any phenomena over the world without making reductions of the data to some standard state of activity.

For the present purpose to treat with the general aspect of the characteristics of amplitude of Sq, the following three criteria are allowable,

- (1). Amplitude difference between all days' mean and calm days' one is to be neglected.
- (2). Solar influence can be generally deduced from the linear expression, $C_n^{N(E)} = C_{n,0}^{N(E)} (1 + m \cdot S)$, $m = 0.58 \cdot 10^{-2}$, while for east components at Kakioka and Haranomachi, $m = 0.38 \cdot 10^{-2}$.
- (3). Fourier coefficients are satisfactorily taken up to the 4th or 5th harmonic.

In order to check the third condition an example of the result of synthetic process of Fourier series is shown in Fig. 64 for east-component at Kakioka. As seen from

Table 24(A). Harmonic analysis of Sq of earth-currents. $N = \sum_n C_n^N \sin(nt + \alpha_n)$, $E = \sum_n C_n^E \sin(nt + \beta_n)$.

Positive direction of currents : northward and eastward.

Unit : mV/km and degree.

\bar{S} : Annual mean sunspot numbers during the interval of observation.

Place	ϕ	λ	C_1^N	C_2^N	C_3^N	C_4^N	α_1	α_2	α_3	α_4	C_1^E	C_2^E	C_3^E	C_4^E	β_1	β_2	β_3	β_4	
Alaska	Fairbanks	65° 54' N	147° 48' W	0.7	6.0	1.5	0.7	90	308	221	355	3.1	2.9	0.4	0.2	227	108	21	300
Canada	Chesterfield	63° 20' N	90° 42' W	0.5	4.2	0.6	0.2	282	76	231	76	4.2	3.0	0.4	0.4	56	252	75	336
Europe	Toledo	39° 53' N	0° 03' W	0.067	0.136	0.085	0.027	77	314	132	349	0.092	0.183	0.217	0.119	256	333	142	321
	Ebro	40° 49' N	0° 33' E	5.34	9.02	3.84	1.07	141	296	124	335	2.09	3.63	1.41	0.38	231	117	306	171
U. S. A.	Tucson	32° 15' N	110° 50' W	0.79	1.51	0.95	0.33	79	272	119	339	0.33	0.68	0.37	0.13	4	188	94	314
South America	Huancayo	12° 03' S	75° 20' W	0.77	0.63	0.32	0.09	350	168	358	217	0.88	0.74	0.39	0.13	166	352	187	35
	San Miguel	34° 33' S	58° 44' W	3.11	2.49	1.66	0.40	48	108	310	292	2.67	2.60	0.77	1.66	85	86	43	312
Saghalien	Toyohara	46° 58' N	142° 45' E	0.44	0.52	0.66	0.15	113	296	84	266	1.00	1.79	1.62	0.57	347	202	44	253
Japan and South-West Pacific region	Memambetsu	43° 55' N	144° 12' E	0.56	0.95	1.01	0.30	44	256	76	285	0.26	0.42	0.52	0.12	339	238	59	259
	Nemuro	43° 20' N	145° 35' E	13.1	7.9	7.8	6.3	350	313	275	226	10.3	6.2	7.0	4.7	175	134	95	43
	Morioka	39° 42' N	141° 01' E	1.12	2.75	2.14	0.56	331	225	46	261	3.32	3.36	2.53	0.29	290	167	357	192
	Haranomachi	37° 37' N	140° 56' E	1.44	1.53	1.46	0.50	84	293	113	310	1.44	1.20	1.09	0.38	287	148	317	155
	Kakioka	36° 14' N	140° 11' E	0.36	1.12	1.21	0.38	56	241	71	268	4.50	5.31	3.38	0.89	294	186	12	205
	Owashi	34° 04' N	136° 12' E	1.58	0.83	0.87	0.26	15	232	61	266	1.04	0.58	0.67	0.25	282	182	323	90
	Kanoya	31° 25' N	130° 53' E	0.37	0.24	0.66	0.25	22	263	59	259	1.34	0.58	0.79	0.36	229	106	290	115
	Ishigaki	24° 20' N	124° 10' E	3.3	0.5	1.8	0.7	302	263	192	198	3.1	1.1	1.0	0.6	77	34	71	6
Australia	Watheroo	30° 19' S	111° 53' E	0.159	0.333	0.195	0.048	65	223	54	214	0.0027	0.0375	0.1700	0.0068	345	42	241	42

Table 24 (B).

Place		Interval	Character of adopted days	Time	\bar{S}
Alaska	Fairbanks	Oct., 1932- Sep., 1933	all days	150°W. M. M. T.	9
Canada	Chesterfield	1932~1933 (81 days)	calm days	90°W. M. M. T.	9
Europe	Toledo Ebro	1948 1914~1918	all days calm days	G. M. T. G. M. T.	136 60
U. S. A.	Tucson	1939~1940	calm days	105°W. M. M. T.	79
South America	Huancayo San Miguel	1927~1929 1951~1952	all days all days	75°W. M. M. T.	71 50
Saghalien	Toyohara	1934~1936			42
Japan and South-West Pacific region	Memambetsu	1950~1953			50
	Nemuro	Jan. -Feb., 1943			(21)
	Morioka	1947			152
	Haranomachi	1950	all days	135° E. M. M. T.	84
	Kakioka	1934~1941			69
	Owashi	1947			152
	Kanoya	1950			84
	Ishigaki	Sep. -Oct., 1941			(56)
Australia	Watheroo	1924~1927	all days	120° E. M. M. T.	49

the figure the third condition may be allowable for an ordinary synthesis of harmonic series, while the other two criteria have been already stated so as to be acceptable.

Table 25 is thus prepared for the estimated amplitudes $C_{n,o}^N$ and $C_{n,o}^B$, which would manifest themselves when S were absent, provided that the second connection is valid up to the extreme value when $S=0$.

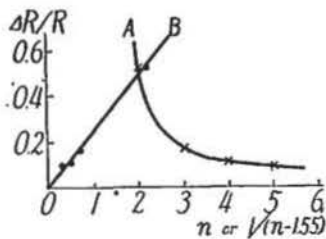


Fig. 64. Relative errors of synthetic values of Fourier coefficients of S_q due to neglected higher harmonics. (East-component at Kakioka)

R : Sum of hourly absolute values of the daily variation.

ΔR : Sum of absolute values of differences between observed hourly values and those of synthetic values up to the n th harmonic.

$A: (\Delta R/R, n)$, $B: (\Delta R/R, 1/\sqrt{n-155})$.

2. Linear relationship between $C_{n,o}^N$ and $C_{n,o}^B$

It is in regard to the daily vector hodograph that in the previous paragraphs we have treated with the principal direction of earth-currents. So it may be natural to retouch here the same problem taking individual harmonic wave into consideration.

Table 25. Values of $C_{n,o}^2$.
unit : mV/km and γ . p : N, E, X and Y, respectively.

Place	$C_{1,0}^N$	$C_{2,0}^N$	$C_{3,0}^N$	$C_{4,0}^N$	$C_{1,0}^E$	$C_{2,0}^E$	$C_{3,0}^E$	$C_{4,0}^E$	$C_{1,0}^X$	$C_{2,0}^X$	$C_{3,0}^X$	$C_{4,0}^X$	$C_{1,0}^Y$	$C_{2,0}^Y$	$C_{3,0}^Y$	$C_{4,0}^Y$
Fairbanks	0.7	5.7	1.4	0.7	2.9	2.8	0.4	0.2								
Chesterfield	0.5	3.8	0.6	0.2	4.0	2.9	0.4	0.4	17.2	14.3	2.4	0.9	5.4	11.9	3.3	2.3
Toledo	0.037	0.076	0.045	0.015	0.051	0.102	0.121	0.066	5.5	2.5	0.3	0.6	9.5	7.3	4.0	1.1
Ebro	3.96	6.69	2.85	0.78	1.55	2.69	1.05	0.28	3.0	1.2	1.3	0.8	9.5	8.5	5.0	1.6
Tucson	0.54	1.04	0.65	0.23	0.23	0.47	0.25	0.09	1.6	2.5	1.4	0.4	8.5	8.3	4.2	1.4
Huancayo	0.55	0.45	0.23	0.06	0.62	0.53	0.28	0.09	3.2	1.6	9	3	60	35	18	3
San Miguel	2.41	1.93	1.29	0.21	2.06	2.02	0.60	0.90					9.7	6.5	3.6	0.9
Toyohara	0.35	0.42	0.53	0.12	0.81	1.45	1.31	0.46	5.8	5.2	3.2	1.1				
Memambetsu	0.43	0.74	0.78	0.23	0.20	0.33	0.40	0.09								
Morioka	0.60	1.46	1.14	0.30	1.77	1.79	1.35	0.15								
Haranomachi	0.97	1.03	0.98	0.34	1.09	0.91	0.83	0.29								
Kakioka	0.26	0.80	0.86	0.27	3.57	4.21	2.68	0.71	1.3	3.1	2.5	0.7	8.8	7.2	4.6	1.4
Owashi	0.84	0.44	0.46	0.14	0.71	0.31	0.42	0.13								
Kanoya	0.25	0.16	0.44	0.17	0.90	0.39	0.53	0.24								
Nemuro	10.8	6.5	6.4	5.2	8.5	5.1	5.8	3.9								
Ishigaki	2.5	0.4	1.4	0.5	2.3	0.8	0.8	0.5								
Watheroo	0.124	0.259	0.152	0.037	0.0021	0.0292	0.0132	0.0053	3.8	1.9	0.6	0.2	8.9	8.7	3.8	1.1

As seen in Fig. 65 the connection between $C_{n,o}^N$ and $C_{n,o}^E$ is approximately linear, as a whole, and stations can be classified into three groups from a standpoint of degree

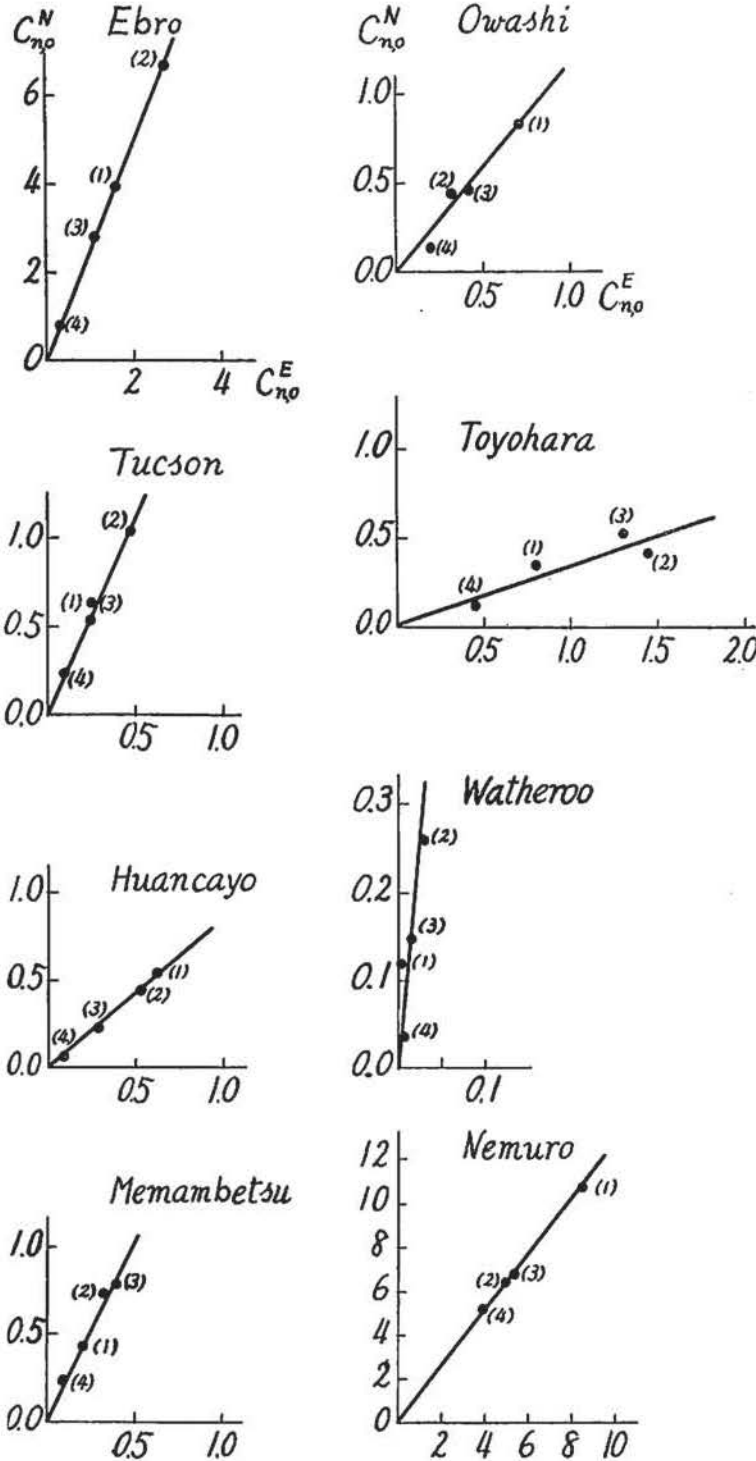


Fig. 65. Linear relationship between $C_{n,o}^E$ and $C_{n,o}^N$. -First group.

of linearity.

(i). *First group:*

First of all the best linearity can be seen, and in other words, each wave persuades its principal axis of the elliptic hodograph in nearly the same direction. And the most predominant wave at any station is common for both east- and north-component as given in Table 25 or Fig. 65. The stations which belong to this group are as follows; Toyohara, Memambetsu, Nemuro, Owashi, Watheroo, Ebro, Tucson and Huancaayo.

(ii). *Second group:*

This group is distinguished from the first group in the following point that some one wave, practically the first wave only, deviates remarkably below the straight line determined by the other waves. Morioka, Hara-

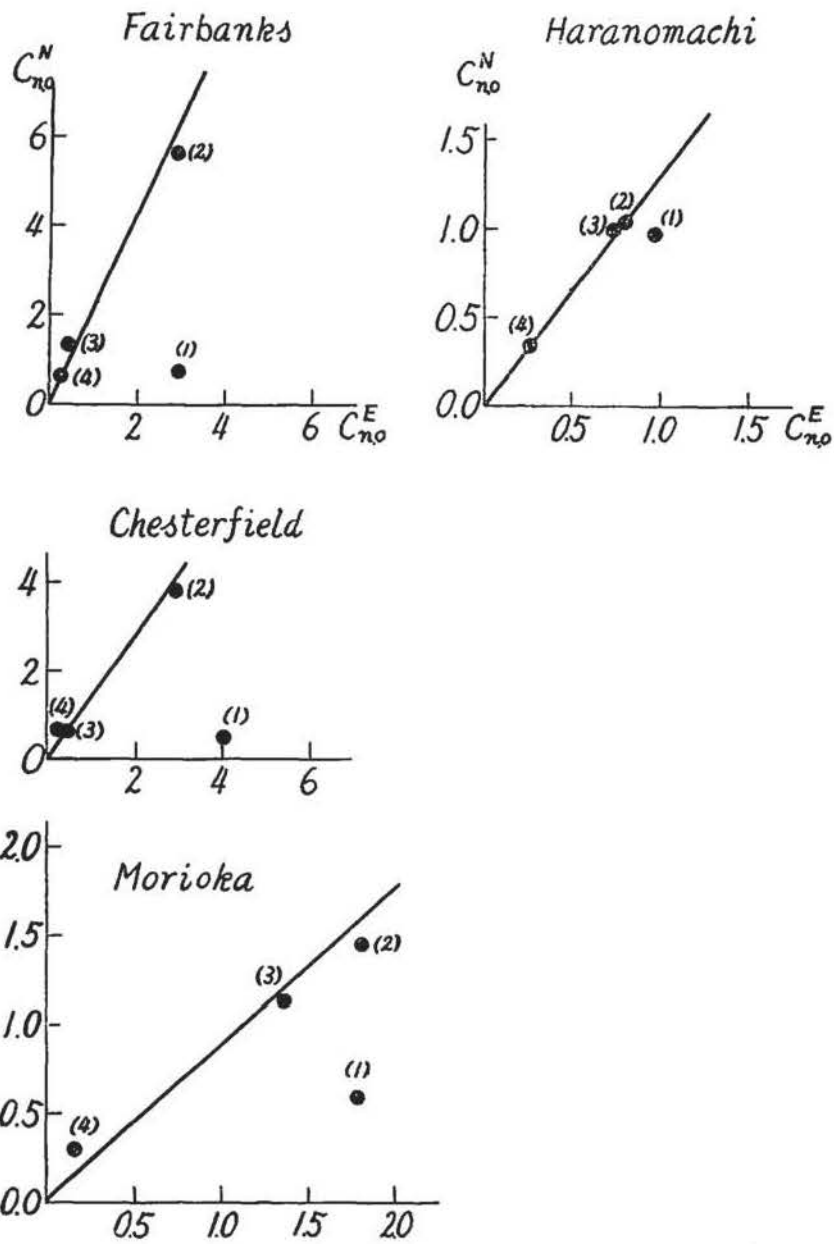


Fig. 65. Linear relationship between $C_{n,o}^E$ and $C_{n,o}^N$ -Second group.

nomachi, Fairbanks and Chesterfield belong to this group. The most predominant wave is diurnal for all east components, but not always so for north-component. So the vector of the first wave exceptionally approaches to the east-west direction.

(iii). *Third group*: This is of less definite linear distribution as compared with the other two groups, and the most predominant wave appears independently of the base line direction. Kakioka, Kanoya, Ishigaki, San Miguel and Toledo belong to this group.

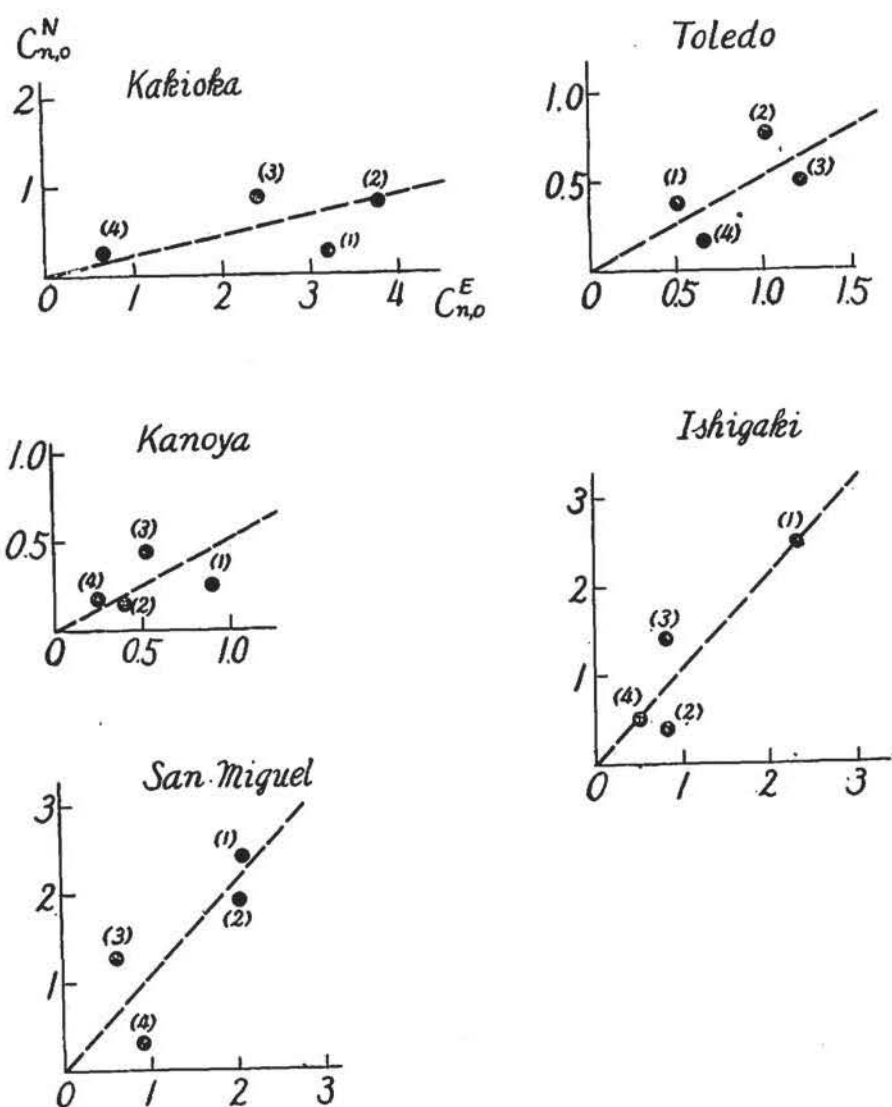


Fig. 65. Linear relationship between $C_{n,0}^N$ and $C_{n,0}^E$ -Third group.

As to the spatial distribution of these three groups, it is to be remarked that the second group seems to appear frequently in both high and middle latitudes especially $30^{\circ}\sim 40^{\circ}$ parallels. In Japan and her vicinity it distributes from the north to south in the successive order of the first, second and third group except for Owashi. The mode of distribution may relate to the electric state of the underground structure, but at some middle latitude stations at least, it is probably responsible to some extent for the irregular distribution of foci of Sq current system. For example, at Kakioka the annual mean state of Sq is remarkably controlled by the corresponding mode of appearance of the first and second waves in winter as shown in Fig. 66, while higher

waves of $n \geq 3$ are independent of any season. As to the higher latitude distribution of the second group, S_D current system may be taken into consideration.

At any rate, it may be pointed out

that the statement said above becomes necessarily when minute features of the principal direction of earth-currents are to be examined for some quantitative discussions.

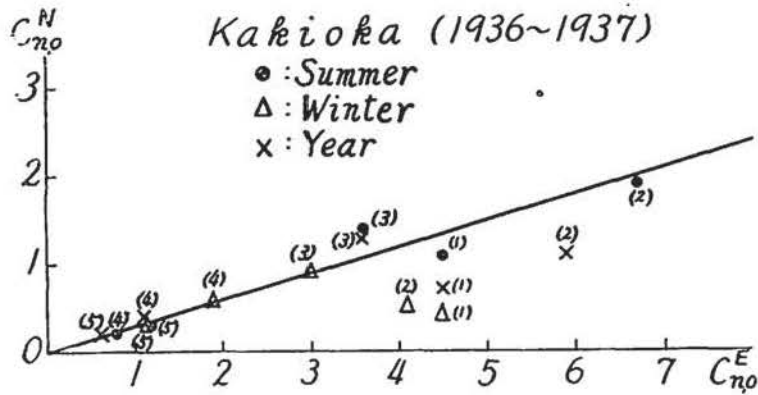


Fig. 66. Seasonal change of correlation between $C_{n,0}^N$ and $C_{n,0}^E$ at Kakioka, 1936~1937.

3. *Locality of $R_{n,0} = \sqrt{C_{n,0}^N{}^2 + C_{n,0}^E{}^2}$ and apparent resistivity ρ_a*

For the convenience to treat with the first approximate features of localities of amplitudes, the resultant $R_{n,0} = \sqrt{C_{n,0}^N{}^2 + C_{n,0}^E{}^2}$ is examined instead of treating separately with $C_{n,0}^N$ or $C_{n,0}^E$ putting any consideration about inhomogeneity of the earth's conductivity aside. As seen in Table 26, magnitude of $R_{n,0}$ is of order of some millivolts per kilometer at most except for exceptionally small values at Toledo and large ones at Nemuro, and as regards the average $R_{n,0}$ no appreciable difference can be seen among three groups of stations mentioned above. At Huancayo, where geomagnetic Sq manifests a well-known equatorial type of variation with large amplitude, one can find no corresponding large $R_{n,0}$ as compared with others, which may strongly suggest an underground structure with sufficient high electric conductivity so as to give rise to rather small amplitude of earth-currents. As a reference of a general conception about the magnitude of $R_{n,0}$, average values for 12 middle latitude stations, except for Fairbanks, Chesterfield, Nemuro, Ishigaki, and Huancayo in Table 26, are given in Table 27.

In view of the well-known electromagnetic induction theory of earth-currents within the earth with uniform conductivity, the amplitude ratio of the horizontal component of electric field E_x to that of magnetic field H_y perpendicular to the x -axis can be expressed by the following simple equation,

Table 26. $R_{n,o} = \sqrt{C_{n,o}^N + C_{n,o}^H}$ and $H_{n,o} = \sqrt{C_{n,o}^X + C_{n,o}^Y}$.

Place	(mV/km)				(γ)			
	$R_{1,0}$	$R_{2,0}$	$R_{3,0}$	$R_{4,0}$	$H_{1,0}$	$H_{2,0}$	$H_{3,0}$	$H_{4,0}$
Fairbanks	3.0	6.4	1.5	0.7				
Chesterfield	4.0	4.8	0.7	0.4	18.0	18.6	4.1	2.5
Toledo	0.063	0.126	0.141	0.069	11.0	7.7	4.0	1.2
Ebro	4.25	7.20	3.04	0.83	9.9	8.6	5.2	1.8
Tucson	0.59	1.14	0.69	0.25	8.6	8.7	4.4	1.4
San Miguel	3.17	2.84	1.42	0.95				
Toyohara	0.88	1.51	1.42	0.48	11.3	8.3	4.8	1.4
Memambetsu	0.47	0.81	0.88	0.25				
Morioka	1.87	2.32	1.77	0.34				
Haranomachi	1.46	1.37	1.28	0.45				
Kakioka	3.58	4.29	2.81	0.76	8.9	7.8	5.2	1.6
Owase	1.11	0.53	0.62	0.19				
Kanoya	0.93	0.40	0.68	0.29				
Nemuro	1.37	8.3	8.6	6.5				
Ishigaki	3.4	0.9	1.6	0.7				
Watheroo	0.124	0.261	0.153	0.038	9.7	8.9	3.8	1.1
Huancayo	0.84	0.69	0.36	0.11	68	38	20	4

Table 27. Mean values of $R_{n,o}$ and $H_{n,o}$. $\bar{R}_{n,o}$: Mean for 12 stations. $\bar{H}_{n,o}$: Mean for 6 stations.

$$E_x/H_y = \sqrt{\rho/2T}, \quad \rho = 1/\sigma,$$

T	$\bar{R}_{n,o}$	$\bar{H}_{n,o}$	$\bar{R}_{n,o}/\bar{H}_{n,o}$
hr	mV/km	γ	
24	1.54	9.9	$0.155 \cdot 10^5$
12	1.90	8.3	0.229
8	1.24	4.6	0.269
6	0.41	1.4	0.293

where T is a period of variation and σ the uniform conductivity of the earth. The conductivity σ , or specific resistance ρ of the earth is not practically uniform at all, but may be a complex

function of space co-ordinates x , y , z and generally even time, although for the mathematical convenience σ is frequently assumed in a tensor form. When the earth is assumed to consist of several horizontal layers with respective uniform conductivity, the matter becomes simpler; for example, in the case of two horizontal layers the amplitude ratio E_x/H_y and phase difference θ are expressed as follows, if it is treated as a two dimensional problem^[63],

$$E_x/H_y = \sqrt{\rho_1/2T} \cdot F(\rho_1, \rho_2, h, T) \equiv \sqrt{\rho_a/2T},$$

$$\tan\theta = (1 - 2Ke^{-y} \sin y - K^2e^{-2y}) / (1 + 2Ke^{-y} \sin y - K^2e^{-2y}),$$

$$F(\rho_1, \rho_2, h, T) = (1 + 2Ke^{-y} \cos y + K^2e^{-2y})^{1/2} / (1 - 2Ke^{-y} \cos y + K^2e^{-2y})^{1/2},$$

$$K = (\sqrt{\rho_2} - \sqrt{\rho_1}) / (\sqrt{\rho_2} + \sqrt{\rho_1}), \quad y = 4\pi h / \sqrt{\rho_1 T},$$

where ρ_1 and ρ_2 are specific resistances of the upper layer and substratum, respectively, and h the thickness of the upper layer and ρ_a apparent resistivity called hereafter. When T is sufficiently large, namely, y is so small, the ratio E_x/H_y is mainly controlled by the presence of substratum and *vice versa*. The phase difference can take any value within the limit of $0 - \pi/2$ by suitable combination of three quantities, ρ_1 , ρ_2 and h , while for the uniform earth the phase difference takes a constant value $\pi/4$.

On the other hand some available geomagnetic data at hands corresponding to that of earth-currents are given in Table 25 and Table 28, where $C_n^{X(Y)} = C_{n,0}^{X(Y)}(1 + m.S)$, $m = 0.58 \cdot 10^{-2}$ is used for the all reductions expect $m = 0.38 \cdot 10^{-2}$ at Kakioka. At Tucson, however, they are given for 1919~1920 because of no corresponding available data in our hands, during which interval sunspot number shows a similar phase of the cycle as that in the interval 1939~1940. The value of $H_{n,0} = \sqrt{C_{n,0}^{X^2} + C_{n,0}^{Y^2}}$ and the average for the six middle latitude stations excluding Chesterfield and Huancayo are given in Table 26 and Table 27.

Table 28. Harmonic analysis of geomagnetic Sq field, $X = \sum_n C_n^X \sin(nt + \delta_n)$,
 $Y = \sum_n C_n^Y \sin(nt + \gamma_n)$. Unit: γ and degree.

Place	C_1^X	C_2^X	C_3^X	C_4^X	C_1^Y	C_2^Y	C_3^Y	C_4^Y	δ_1	δ_2	δ_3	δ_4	γ_1	γ_2	γ_3	γ_4	Positive direction	Period
Chesterfield ^[55]	18.1	15.0	2.5	0.9	5.7	12.5	3.5	2.4	80	198	342	169	230	140	156	341	N W	Oct., 1932- Sep., 1933 (calm days)
Toledo ^[56]	9.8	4.5	0.6	1.0	17.1	13.1	7.1	1.9	48	209	291	84	42	210	51	255	N E	1948(all days)
Ebro ^[57]	4.1	1.6	1.8	1.1	12.8	11.4	6.7	2.2	99	236	199	61	35	220	53	246	N E	1914-1918 (calm days)
Tucson ^[58]	2.4	3.6	2.1	0.5	12.5	12.1	6.1	2.0	99	328	172	34	1194	26	234		N E	1919-1920 (calm days)
Toyohara ^[59]	7.2	6.4	4.0	1.3	12.0	8.1	4.5	1.1	100	328	161	18	217	46	226	56	N W	1934-1936 (all days)
Kakioka ^[60]	1.7	3.9	3.2	0.9	12.3	10.0	6.4	2.0	48	335	158	7	211	42	227	68	N W	1934-1941 (all days)
Watheroo ^[61]	4.9	2.4	0.8	0.2	11.4	11.2	4.7	1.4	26	247	48	53	184	358	194	12	N E	1924-1927 (all days)
Huancayo ^[62]	45	22	12	4	85	49	25	3	343	122	342	188	272	102	247	340	N E	1927-1929 (all days)

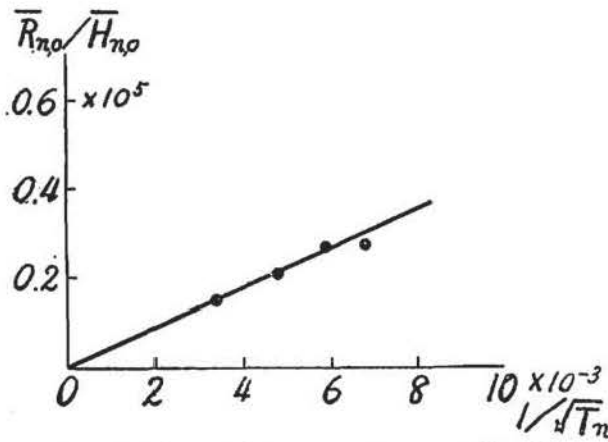


Fig. 67(B). Relationship between $\bar{R}_{n,o}/\bar{H}_{n,o}$ and $1/\sqrt{T_n}$ for Sq.

At any rate, taking a simple theoretical result mentioned above into consideration it was tried to see in what manner $R_{n,o}/H_{n,o}$ does correlate to $1/\sqrt{T_n}$, and the result is graphically shown in Fig. 67(A). Here the observed values of $H_{n,o}$ at Toyohara and Kakioka are assumed to be equal to $H_{n,o}$'s which would be observed

at Memambetsu and the other all Japanese earth-current stations, respectively. And also for Fairbanks and San Miguel are used $H_{n,o}$'s observed at Chesterfield and the middle latitude average value given in Table 27, respectively. As seen in the figures, as a whole, there is a nearly linear correlation between $R_{n,o}/H_{n,o}$ and $1/\sqrt{T_n}$, although unfortunately, the present material of earth-currents and geomagnetic forces are not always supplied from the same stations, and also intervals of observations or epochs of the sunspot activity differ each other at some stations. As far as the average values given in Table 28 are concerned, a fairly good connection can be found as shown in Fig. 67(B). So it is confirmed that the amplitude ratio $R_{n,o}/H_{n,o}$ is proportional to $1/\sqrt{T_n}$ for the first approximation in many places over the world in spite of their supposed different modes of structure of the ground as far as such a range of period that covers those of principal harmonics of the Sq variation is concerned. Nevertheless, at some places, where there is seen scarcely a linear relation, we may have such special ground structures that, say, for the two layers' structure ρ_2 is very larger than ρ_1 and the ratio $R_{n,o}/H_{n,o}$ shows no dependency on $1/\sqrt{T_n}$. On the contrary when $\rho_2 \ll \rho_1$ and y is very small, the amplitude ratio may become proportional to $1/T_n$, showing a concave curve in Fig. 67(A).

4. Apparent resistivity ρ_a and earth-resistivity ρ_{obs} near the earth's surface

Assuming such a simple structure of the earth as said above, ρ_a 's are calculated from $R_{n,o}/H_{n,o} = \sqrt{\rho_a/2T_n}$ and given in the second column of Table 29. They are of order of $10^4 \Omega \cdot \text{cm}$ at nine stations out of fifteen, and as small as $3 \sim 4 \cdot 10^3 \Omega \cdot \text{cm}$ at Huancayo and Toledo. The average value of ρ_a corresponding to Fig. 67(B) gives

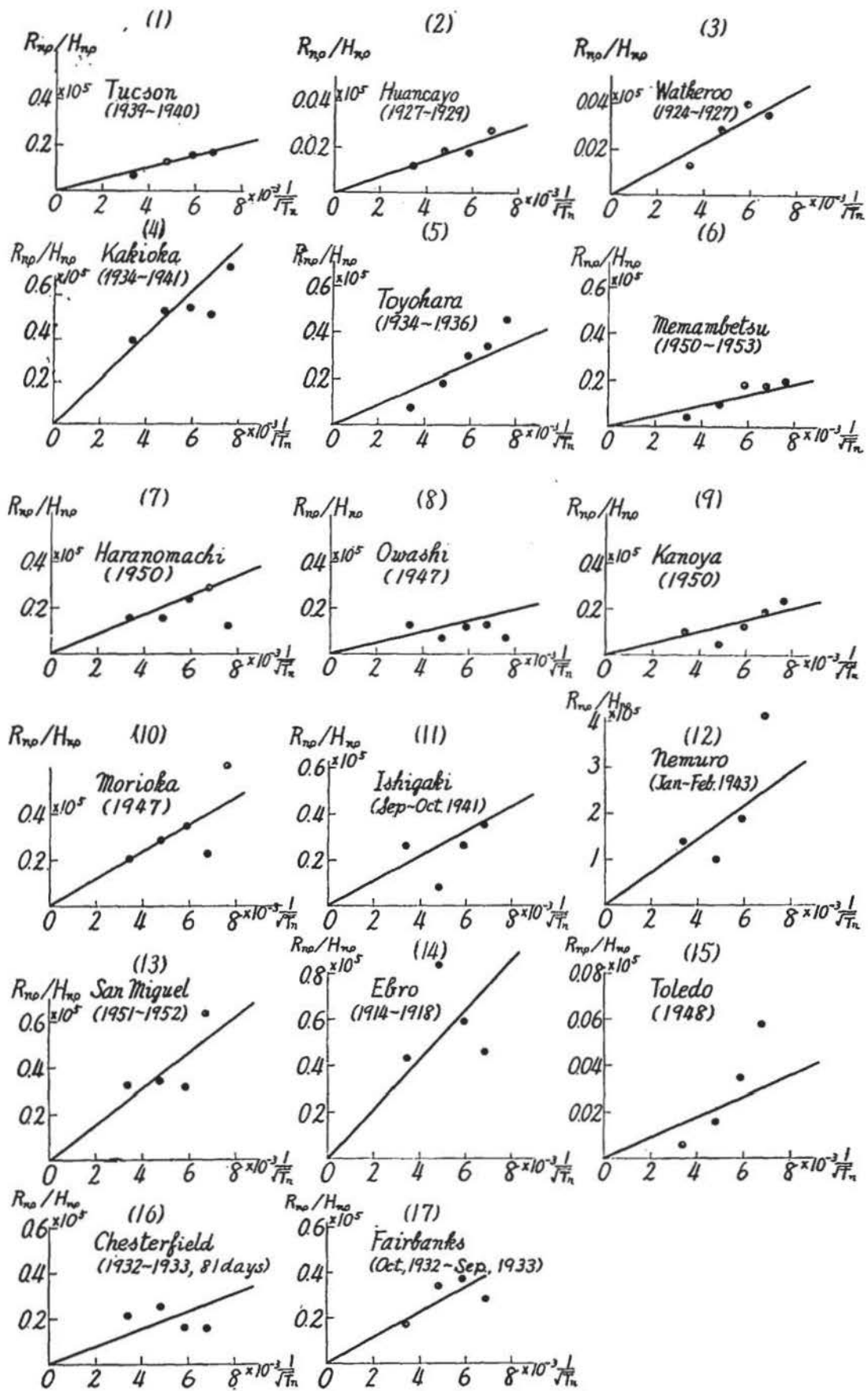


Fig. 67(A). Relationship between $R_{n,o}/H_{n,o}$ and $1/\sqrt{T_n}$ for Sg at each station.

Table 29. Estimated apparent resistivity ρ_a and earth-resistivity ρ_{obs} measured by Wenner-Gish-Looney method.

Station	ρ_a Ω. cm	ρ_{obs} Ω. cm
Fairbanks	$6.4 \cdot 10^4$	
Chesterfield	$2.9 \cdot 10^4$	
Toledo ^[64]	$0.4 \cdot 10^3$	$2 \cdot 10^3$
Ebro ^[65]	$2.3 \cdot 10^5$	$11 \cdot 10^3$
Tucson ^[66]	$1.5 \cdot 10^4$	$3 \cdot 10^3$
Toyohara	$3.9 \cdot 10^4$	$4 \cdot 10^3$
Memambetsu	$1.1 \cdot 10^4$	
Morioka	$6.7 \cdot 10^4$	$4 \cdot 10^3$
Haranomachi	$3.8 \cdot 10^4$	$5 \cdot 10^3$
Kakioka	$1.9 \cdot 10^5$	$14 \cdot 10^3$
Owashi	$1.2 \cdot 10^4$	
Kanoya	$1.4 \cdot 10^4$	$33 \cdot 10^3$
Huancayo ^[67]	$0.3 \cdot 10^3$	$13 \cdot 10^3$
Watheroo ^[68]	$0.6 \cdot 10^3$	$15 \cdot 10^3$
San Miguel	$1.2 \cdot 10^5$	

$4 \cdot 10^4 \Omega\text{cm}$. The remarkable variety of ρ_a indicates clearly the locality of universal earth-currents.

On the other hand, at some of the stations considered here have been carried out some earth-resistivity surveys with different scale and depth of penetration, but almost the same Wenner-Gish-Looney method was used. These observed earth-resistivities, denoted by ρ_{obs} here, are given in the third column of Table 29, of which effective depth corresponding to the inner electrode span, a , is about 200 meters. Of course,

ρ_{obs} is generally different in different direction and depth, sometimes largest values being crowded in relatively small area in the vicinity of a station. In practice, however, most of surveys have been carried out to the effective depth corresponding to $a=200\sim300$ meters at most. Now ρ_{obs} at $a=200$ meters is assumed to be more or less representative for the

average state of ρ_{obs} near the earth's surface in relatively wide area around the station. It becomes then interesting to know whether or not any connection does exist between ρ_a and ρ_{obs} , the result being graphically shown in Fig. 68 in logarithmic scale. Excepting Huancayo and

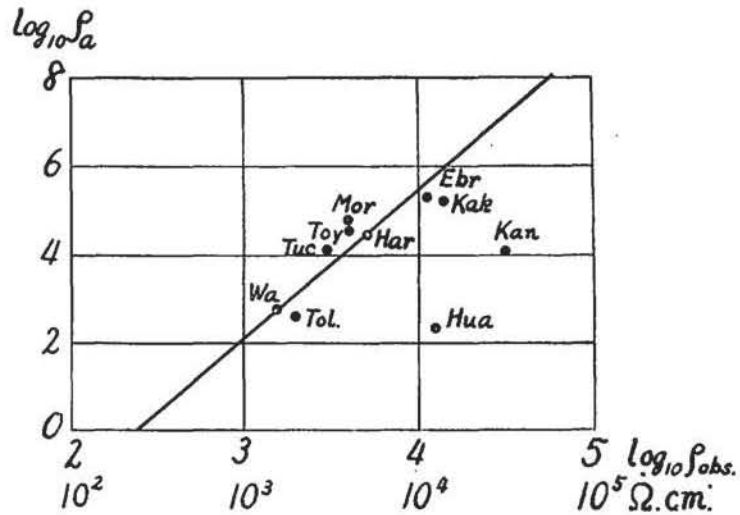


Fig. 68. Relationship between ρ_a and observed earth-resistivity ρ_{obs} .

Kanoya, remaining eight points approximately fall on a straight line, ρ_{obs} 's at these two stations being as large as about ten times those expectable from this linear expression. As seen from the depth distribution of ρ_{obs} given in Table 30,

Table 30. Earth-resistivity ρ_{obs} at Kanoya. (Wenner-Gish-Looney method)

a	EW	NS
	Ω . cm	Ω . cm
300m	$2.37 \cdot 10^4$	$2.40 \cdot 10^4$
200	3.13	3.61
100	5.12	5.70
70	6.78	6.21
40	6.72	4.40

ρ_{obs} at Kanoya decreases so rapidly with increasing depth that if the upper high resistivity layer be ignored, the average ρ_{obs} of deeper portions may fall to some thousand ohm. cm. This is near to a reasonable magnitude expectable from the figure. ρ_{obs} at Huancayo decreases in a similar way with increasing depth, namely, it attains to $5 \cdot 10^3 \Omega$. cm at about $a=600$ meters and seems further to decrease gradually. So two exceptionally deviated values of both Kanoya and Huancayo would approach to the line in Fig. 68, provided that some plausible ρ_{obs} is taken in place of the present ρ_{obs} corresponding to $a=200$ m. So as far as these stations are concerned, contribution of the uppermost part of the earth to ρ_a may be approximately expressed as follows,

$$\rho_a = 10^{-8.1} \cdot (\rho_{obs})^{3.1} \Omega \text{ cm.}$$

Summarizing the results obtained above, it is found out that there exists a fairly close connection between apparent resistivity ρ_a , presumed from earth-currents

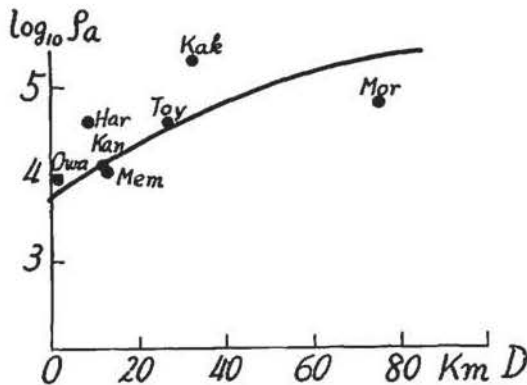


Fig. 69. Variation of apparent resistivity ρ_a with regard to the distance D from the nearest sea-coast to the station, Japan.

and geomagnetic field, and average earth-resistivity ρ_{obs} , observed in the upper portion of the earth up to some hundred meters or more below the surface. And the matter is not of mere chance, but actually the upper portion of the earth near any station may contribute more or less in similar manner to the magnitude of earth-currents observed. Then, it is easy to understand such a well-known experience in applied geophysics, or electric

surveys that magnitude of natural earth-currents observed in a small area, in which geomagnetic potential is considered to be constant, increases with increasing earth-resistivity. It is also natural to expect a systematic distribution of ρ_a , or magnitude of earth-currents in a limited area such as the Japanese Island, of which mountainous portions are probably of higher earth-resistivities and lower near the coast, as a whole. Actually, as shown in Fig. 69, ρ_a increases gradually with increasing distance from the coast. And the large ρ_a at Kakioka is also in consistent with high earth-resistivity observed, which is due to the upper portion of rocky substratum of the Tsukuba mountain block. At any rate, since there has been no synthetic statement about the role of observed earth-resistivity to act upon the observed earth-currents, the results obtained here will be useful not only for the interpretation of earth-currents variations, but also for directions of earth-resistivity measurements, as far as the first approximate considerations of the electric structure of the earth are concerned.

5. *Presumed localities of underground electric structures in some places in Japan*

At last it may be practically interesting to estimate some plausible structure of the shallow part of the underground mass from an electromagnetic point of view. Here, the matter is treated simply as a two-layer problem in two dimensions as mentioned above, and the underground structure will be estimated very roughly by using the amplitude ratio R_n/H_n , because of combining some material for short period variations. Of course, more complicated mathematical treatment may be possible, but it belongs to a multiple values' problem and besides, few observational back grounds for it have been reported. The diagrams, $(R_n/H_n, 1/\sqrt{T_n^-})$, at some stations in Japan are shown in Fig. 70(A)-(D), where at Toyohara⁽⁶⁶⁾ C_n^H/C_n^X is used in place of R_n/H_n , because the average amplitude of the short period variation corresponding to a specified period at Toyohara is given for various kinds of variations of X and east-component. The values marked by black circles in Fig. 70(D) are calculated from nearly periodic variations chosen from many available records. The other short period variations referred are all SSC's, for which T_n 's are taken twice times the duration from the beginning to the maximum value of the geomagnetic horizontal intensity. These figures show that all curves change convexly with increasing $1/\sqrt{T_n^-}$, namely, indicating $\rho_2 \gg \rho_1$,

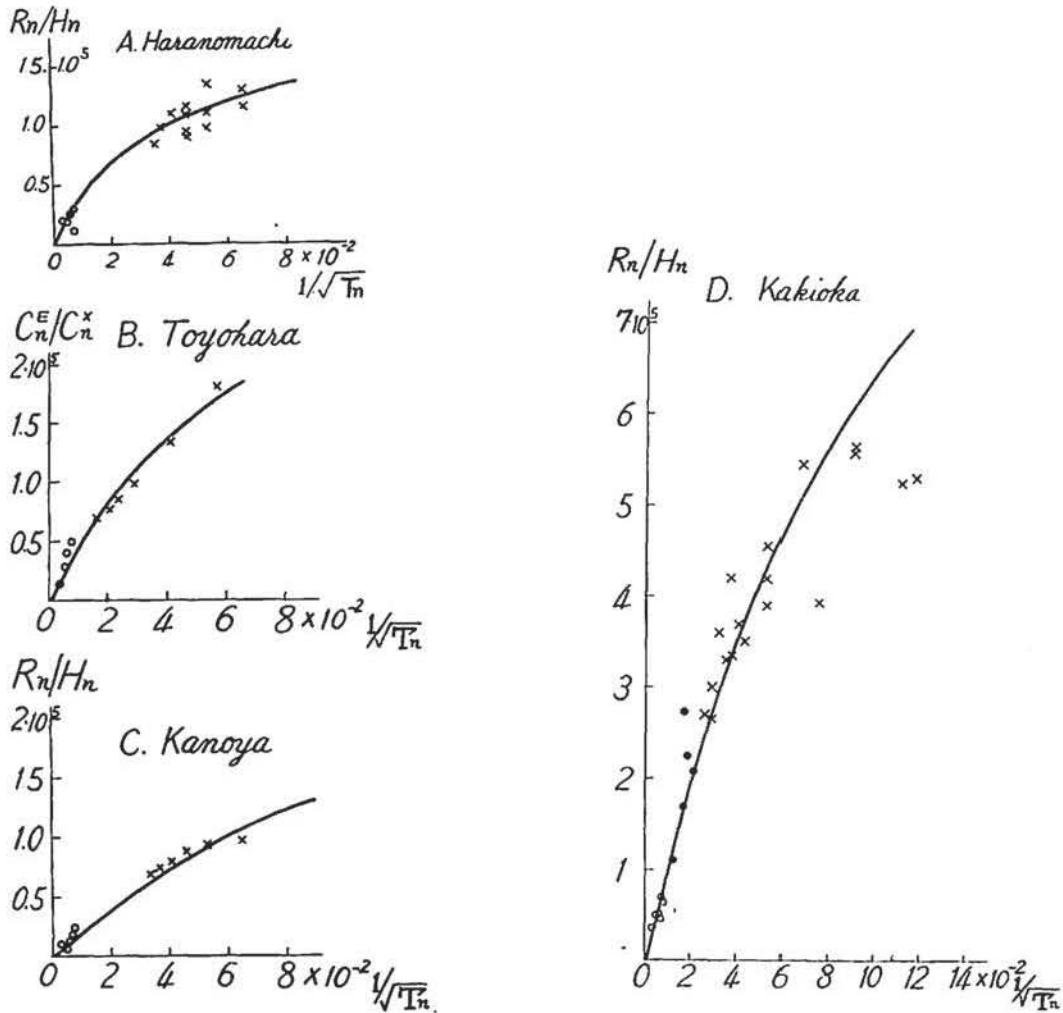


Fig. 70(A)-(D). Relationship between R_n/H_n and $1/\sqrt{T_n}$ at four stations in Japan when both Sq and some short period variations are taken into consideration.

Fig. 70 (D)

while they are approximately linear as already mentioned within the range of period corresponding to those of principal harmonics of Sq. So we may presume more or less reasonably the specific resistance of the substratum ρ_2 from Sq analysis presented here. After some trials, considering the correlation between ρ_α and ρ_{obs} , an adjusted theoretical curve is drawn by a solid curve for each figure of Fig. 70, showing a fairly good agreement with observations.

Although we have no observational evidence to check the plausibility of these quantities obtained from the other geophysical points of view, it may be interesting to note that in the vicinity of Tokyo the propagation velocity of earthquake waves in the upper

Table 31. Presumed values of h , ρ_1 , and ρ_2 in some places in Japan.

Station	h	ρ_1	ρ_2
	km	$\Omega \cdot \text{cm}$	$\Omega \cdot \text{cm}$
Toyohara	5	$2.0 \cdot 10^3$	$55 \cdot 10^3$
Haranomachi	5	1.4	22
Kakioka	6	8.0	200
Kanoya	3	1.0	11

layer of a few kilometers in thickness can be distinguished from that of the lower part⁽⁷⁰⁾. The values of h , ρ_1 and ρ_2 used for calculations are tabulated in Table 31, and it should be remembered that the matter is not

always uniquely determined.

6. *Anomalous amplitude of the harmonic waves of Sq near the sea-coast*

Following the preceding paragraph, here something about irregularities of the distribution of observed points in

Fig. 67 will be treated. In the first place, one can notice that some stations in Japan, such as Kanoya, Ishigaki and etc., show the remarkably small semi-diurnal waves. So if the deviation of observed $R_{2,0}/H_{2,0}$ from the corresponding value $(R_{2,0}/H_{2,0})_0$ on the straight line in the figure be denoted by $\Delta(R_{2,0}/H_{2,0}) = (R_{2,0}/H_{2,0}) - (R_{2,0}/H_{2,0})_0$, the ratio $\Delta(R_{2,0}/H_{2,0}) / (R_{2,0}/H_{2,0})_0$ is almost negative, and monotonously distributed as shown in Fig 71(A) in respect to the distance D measured from the

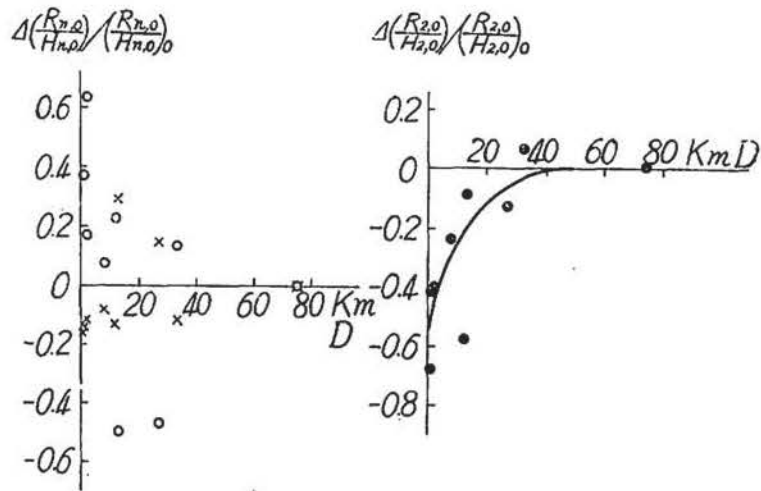


Fig. 71 (A). Variation of $\Delta\left(\frac{R_{2,0}}{H_{2,0}}\right) / \left(\frac{R_{2,0}}{H_{2,0}}\right)_0$ with D in Japan.
 White circle : first wave.
 Cross mark : third wave.
 Black circle : second wave.

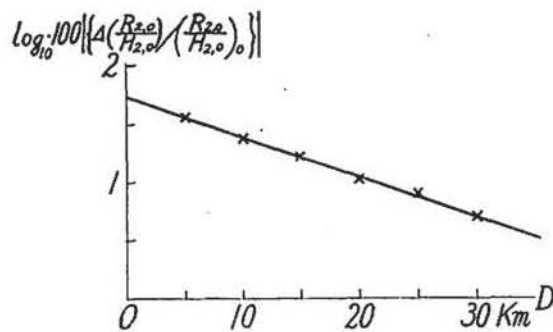


Fig. 71(B). Relation between $\Delta\left(\frac{R_{2,0}}{H_{2,0}}\right) / \left(\frac{R_{2,0}}{H_{2,0}}\right)_0$ and D .

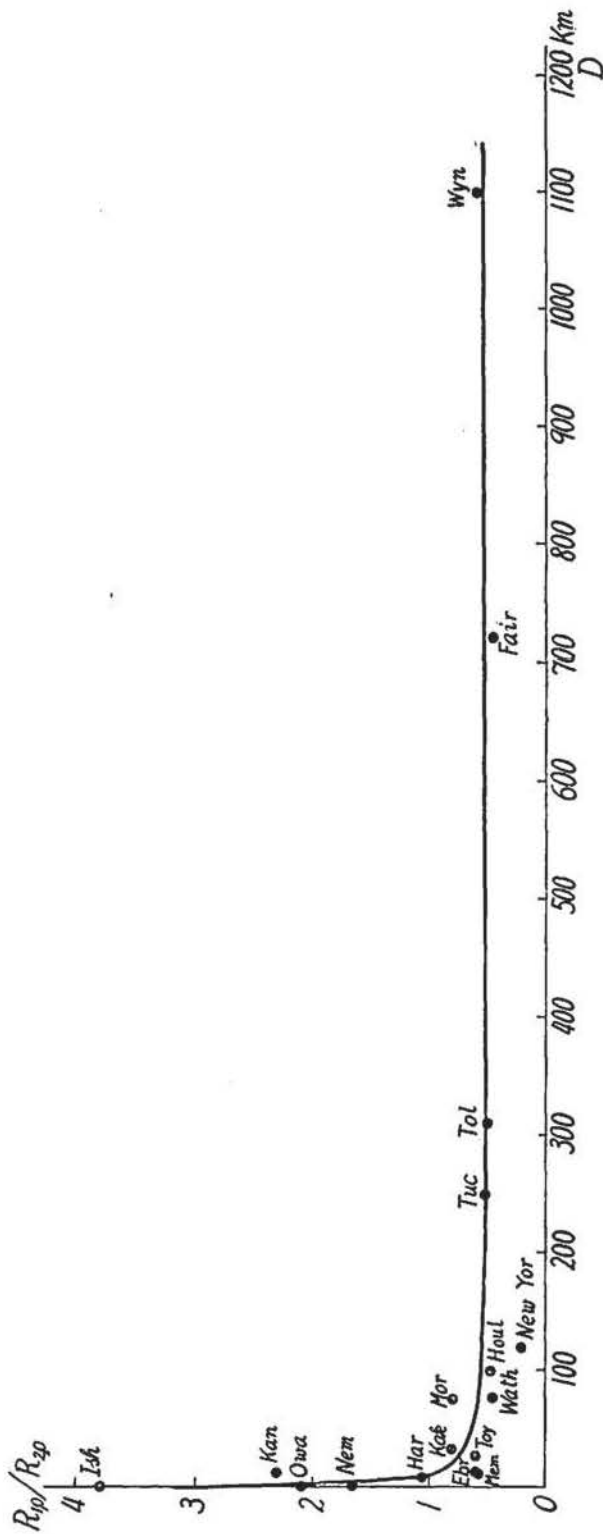


Fig. 72. Variation of $R_{1,0}/R_{2,0}$ with D at several stations in the world.

Wyn : wyamet (U.S.A.)

New Yor : New York (U.S.A.)

Houl : Houlton Me. (U.S.A.)

Fair : Fairbanks (Alaska); Tol ; Toledo (Spain) ; Tuc : Tucson (U.S.A.) ;

Wath : Watheroo (Australia) ; Mor : Morioka (Japan) ; Toy : Toyohara (Saghalien) ;

Kak : Kakioka (Japan) ; Ebr : Ebro (Spain) ; Mem : Memambetsu (Japan) ;

Har : Haranomachi (Japan) ; Nemuro (Japan) ; Owa : Owashi (Japan) ; Kan : Kanoya (Japan) ; Ish : Ishigaki (Japan).

nearest sea-coast to the respective station. The numerical value of the ratio rapidly increases near the sea-coast in a fairly regular form, of which average curve may be expressed approximately as follows as shown in Fig. 71(B),

$$\Delta(R_{2,0}/H_{2,0}) / (R_{2,0}/H_{2,0})_0 = -Ae^{-\gamma \cdot D},$$

$$A=0.54, \quad \gamma=0.078,$$

where the distance D is measured in unit of km. In the second place, however, it is examined in vain to get such a regular distribution as said above for the other waves, showing remarkable fluctuations at some stations. (Fig. 71(A))

On the other hand, the ratio $R_{1,0}/R_{2,0}$ observed in various places over the world is shown in Fig. 72 in order to check the anomalous distribution of the amplitude before-mentioned within more wide range of D . The ratio falls also very rapidly within the interval from the coast to 20~30 km distance, and tends to a nearly constant value $R_{1,0}/R_{2,0} \simeq 0.5$ as far as 1000 km from the coast. Therefore, the anomalous behavior of the second wave is characterized within very small distances from the coast, and so its origin may be attributed to some phenomena related directly with the sea.

In respect to this point it may first lead us to remind of the lunar daily variation of earth-currents, of which available data seem to be so scanty at present to establish

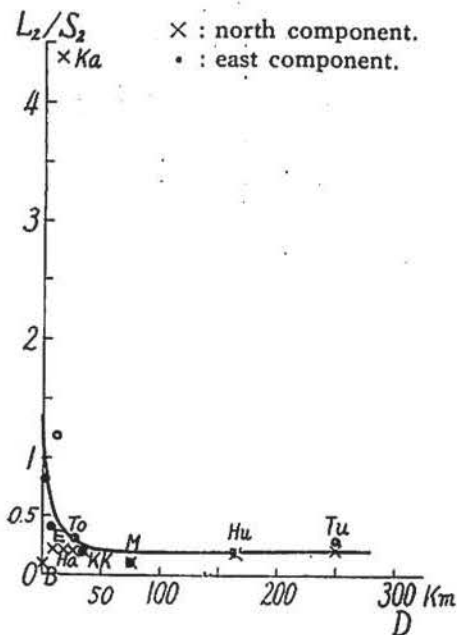


Fig. 73. Relation of L_2/S_2 of earth-currents to D .

any definite picture of the phenomena. However, it is a fact that the value of L_2/S_2 , ratio of the semidiurnal amplitude of the lunar daily variation to that of S_q is only about 1/15 for the geomagnetic field, while for earth-currents it has been known to be as large as three or four times the former. Furthermore, the results of recent observations given in Table 32 or Fig. 73 strongly suggest that the lunar daily variation of earth-currents should be discussed first of all from the local standpoint of view, taking the relative distribution of land and sea into consideration. In other words, this suggests also some similar local origins for the anomalous

amplitude of the second wave of S_q , since these systematic anomalous effects can be found only for the semi-diurnal wave and of comparatively large magnitude. In the following some possible explanations will be put forth.

The first is that the solar semi-diurnal ocean tide in the permanent geomagnetic field

Table 32. L_2/S_2 at several stations over the world.

Station	NS	EW
Tucson ⁽⁷¹⁾	0.2	0.3
Huancayo ⁽⁷¹⁾	0.2	0.2
Ebro ⁽⁷²⁾	0.2	
Kakioka ⁽⁷³⁾	0.2	0.2
Toyohara ⁽⁷⁴⁾	0.2	0.3
Beppu ⁽⁷⁴⁾	(0.1)	0.8
Kanoya ⁽⁷⁵⁾	4.4	1.2
Haranomachi ⁽⁷⁵⁾	0.2	0.4
Morioka ⁽⁷⁵⁾	0.1	0.1

produces the corresponding e. m. f. in the sea, which may have its leakage circuit in the land. The relative amplitude of the solar semi-diurnal component of the tide is about 0.32 when that of lunar semi-diurnal tide is taken as unity, while that of the solar diurnal component is 0.11⁽⁷⁶⁾. So any electric field due to such a kind of origin ought to be most predominant in the semi-diurnal term, the situation being thus favourable to the present problem. The second is that under the same circumstance some electrochemical potential, say, a kind of concentration cell may be formed near the coast due to permeating sea-water into the land, or retarded underground water streaming into the sea. They are subjected to a semi-diurnal change of concentration with raising and falling sea-level. At some stations situated so near the sea-side, remarkable contact potentials can be set up at the electrodes due to direct contact with concentric saline solution of the ground adjacent to them. On the other hand, regarding the motion of the soil liquid the third possible cause is pointed out such as that an appreciable magnitude of so-called streaming potential may be changed, or newly produced under suitable conditions between the sea-coast and the inner part of the land. For example, when the sea-water raises upwards, expectable geomagnetic induction currents may flow nearly westwards in the vicinity of Japan, and at the same time soil liquid may become sufficiently concentrative near the coast to yield on appreciable magnitude of electromotive force which is likely to direct towards less concentrated inner parts of the land.

At any rate, if the proper semi-diurnal wave of earth-currents, say east-component be expressed by $E_2 \cdot \sin(2t + \varphi_2)$, positive sense reckoned eastwards, and that of

local earth-currents said above by $-E_2^1 \sin(2t + \varphi_2^1)$, combined value becomes as follows,

$$e_2 = E_2^0 \sin(2t + \varphi_2^0) - E_2^1 \sin(2t + \varphi_2^1) = E_2 \sin(2t + \varphi_2),$$

$$E_2 = E_2^0 \sqrt{1 - 2(E_2^1/E_2^0) \cos(\varphi_2^0 - \varphi_2^1) + (E_2^1/E_2^0)^2},$$

$$\tan \varphi_2 = \frac{1 - \frac{E_2^1}{E_2^0} \cdot \frac{\sin \varphi_2^1}{\sin \varphi_2^0}}{1 - \frac{E_2^1}{E_2^0} \cdot \frac{\cos \varphi_2^1}{\cos \varphi_2^0}} \cdot \tan \varphi_2^0.$$

On the other hand, at several inland stations far remote from the sea-coast φ_2^0 's are approximately equal to π , and an average phase angle of the solar semi-diurnal wave of the tide is also near π in the vicinity of Japan⁽⁷⁷⁾; the semi-diurnal oscillation of the atmospheric pressure change is known so as to have its two maxima at about 9 hr and 21 hr in local time. Furthermore, concerning observed semi-diurnal phase angles there is found no such a definite connection with D as seen in the case of amplitude distribution (Fig. 25). So we may assume $\varphi_2^0 = \varphi_2^1$, and furthermore when $(E_2^1/E_2^0)^2 < 1$, e_2 can be approximately written as follows,

$$e_2 = E_2^0 (1 - E_2^1/E_2^0) \sin(2t + \varphi_2^0).$$

Hence the amplitude deviation of e_2 from E_2^0 , is given as follows,

$$\frac{e_2 - E_2^0}{E_2^0} = -\frac{E_2^1}{E_2^0}$$

It is natural to consider the decreasing amplitude of E_2^0 with increasing distance D from the sea-coast, and if $E_2^1 = (E_2^1)_{D=0} \cdot e^{-\alpha D}$ is assumed, as seen in the case of permeating water level in the land adjacent to a water channel⁽⁷⁸⁾, then,

$$\frac{e_2 - E_2^0}{E_2^0} = -\frac{(E_2^1)_{D=0}}{E_2^0} \cdot e^{-\alpha D}.$$

This expression may be applicable to an interpretation of observational results for $\Delta(R_{2,0}/H_{2,0})/(R_{2,0}/H_{2,0})_0$, or $R_{1,0}/R_{2,0}$ as far as we confine the event itself to the matter in the vicinity of Japan and neglect supposed small geomagnetic effect due to the local currents said above.

At last, rough estimations of the order of magnitude of possible effects before-mentioned will be made in the following. The induced e. m. f. due to the tidal motion of sea-water is given by

$$E = H \cdot v,$$

where H is the geomagnetic horizontal intensity of 0.3Γ , and v the velocity of rising or falling of the sea-level height, $h = h_2 \sin(2pt + \alpha_2)$. So putting $h_2 = 20$ cm for an average

solar semi-diurnal tide^[78], and conductivity of sea-water $\sigma_s=0.03$ (35% salinity and 10°C), the amplitude of induced e. m. f. E_2^s and current density I_2^s are as follows,

$$E_2^s=0.3 \cdot 2ph \cdot 10^{-9}=8.4 \cdot 10^{-2} \text{ volts,}$$

$$I_2^s=\sigma_s \cdot E_2^s=2.5 \cdot 10^{-13} \text{ Amp.}$$

If I_2^s be assumed to flow uniformly in the ground adjacent to the sea-side, potential difference along a stream line in the ground is

$$E_2^l=I_2^s \cdot \rho_l \cdot L=0.3 \text{ mV/km,}$$

where specific resistance of the ground $\rho_l=10^4 \Omega \cdot \text{cm}$ is assumed, and L the length of a base line. As E_2^s is of order of $0.5 \sim 2 \text{ mV/km}$, $(E_2^s)_{D=0}$ is $0.3 \sim 1.1 \text{ mV/km}$, assuming $(E_2^l)_{D=0}/E_2^s=0.54$. This value is of the same order as E_2^l , but in the ground equal current density as that presumed in the sea is assumed, the conductivity of the latter being very much larger than that of the ground. So, this type of e. m. f. seems to be unsuitable for the sufficient interpretation of the matter.

The electrochemical potential difference due to a concentric cell is given by

$$e=KT \log\left(\frac{C_2}{C_1}\right),$$

where C_2 and C_1 are concentrations of a supposed solution around the corresponding two electrodes, and K a constant specified by the solution, and T the absolute temperature of the solution. Now, when the solution is taken as NaCl and $T=291^\circ$,

$$e=\frac{u_- - u_+}{u_- + u_+} \cdot \frac{R}{F} \cdot T \cdot \log\left(\frac{C_2}{C_1}\right)=11.6 \log_{10}\left(\frac{C_2}{C_1}\right) \text{ (mV).}$$

If we suppose that C is given by

$$C=C_0 e^{-\beta D},$$

where D is expressed in unit of km.

$$\text{So, } C_2/C_1 = \frac{C_0 e^{-\beta D_2}}{C_0 e^{-\beta(D_2+\Delta)}} = e^{\beta \cdot \Delta}.$$

As before-mentioned, say putting $e=0.3 \text{ mV/km}$ and base length $\Delta=1 \text{ km}$, we have

$$\beta=0.06,$$

$$C=C_0 e^{-0.06D}.$$

The value of β is nearly equal to γ in the expression of $\Delta(R_{2,0}/H_{2,0})/(R_{2,0}/H_{2,0})_0$; a plausible explanation may be promised providing more comprehensive material.

T. Terada^[80] has pointed out a possibility that luminous phenomena accompanying destructive sea-waves (Tsunami) may be explained by taking streaming

potential produced in the sea-bottom into account, which is proportional to the difference of water-heads of the high water of a tsunami and normal sea-level. For the present problem similar considerations may be applicable. In some cases meteorological water contained in the water-bearing layer may manifest a horizontal displacement towards the sea-side under the horizontal pressure gradient due to the difference of vertical pressure exerting upon the layer. On the contrary, high sea-water itself may permeate into the land in other circumstances. At any rate, expectable change of streaming potential in the ground due to the varied height of the sea-level may be given by

$$E = \frac{\zeta \cdot D \cdot \rho}{4\pi\eta} \cdot p,$$

where ζ is the kinetic potential (mostly 0.01~0.05 volts), p the total hydrostatic pressure difference, D , ρ and η respectively the dielectric constant, specific resistance, and coefficient of viscosity of the liquid. Taking p equals to the pressure exerting at the depth of sea-water of $h_2=10$ cm, and besides, say, for the ground water, $\zeta=0.03$ volts, $\rho=10^3 \Omega \cdot \text{cm}$, $D=81$ and $\eta=0.01$ ($t=15^\circ$), we have,

$$E=0.2 \cdot 10^{-3} \text{ volts.}$$

This is the same order as that requested from observations, but we have no reliable data to refer concerning actual motion of soil liquid in any horizontal level and some constants considered above. So the value is of very rough estimation at all.

§ 5. Some characteristic features of the disturbance field of earth-currents observed in Japan

1. Introduction

In the previous paragraphs all statements on various characteristics of earth-currents are obliged to be based on Sq field only in order to discuss the problem in a world-wide scale of data, since no systematic material of disturbing field has been published. However, in view of both geophysical interest and inductive nature of earth-currents, a study of the universal earth-currents is to be promoted along the line to analyse and interpret so-called short period variations with regard to their spectrums of period, frequency characteristics of some specified variations and etc. Recently, along this line of investigations various works have been carried on by the members

of our observatory. In this paragraph some newly found characteristics of *SSC* and *SI* changes of earth-currents observed at Kakioka and other stations in Japan will be reported.

2. Preliminary changes of *SSC* and *SI* of earth-currents

[A]. Preliminary change

Both *SSC* and *SI* changes are characterized by their first impulsive movements in geomagnetic field and earth-currents as well as their world-wide appearance. It has been commonly accepted that the first movement of *SSC* starts suddenly from some point on the magnetograph or electrogram, independent of the state of activity at that time. However, in the course of preparing long period material of *SSC*'s for the investigations of their diurnal and seasonal frequencies at Kakioka⁽⁶¹⁾, it was found out that a

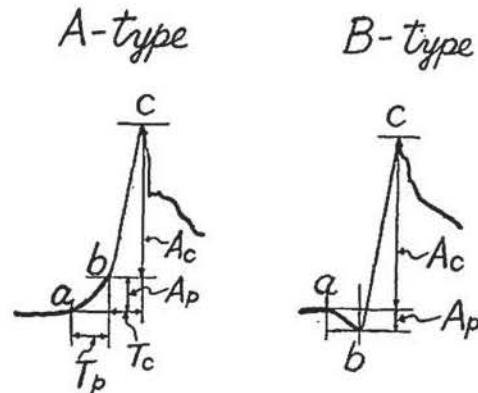
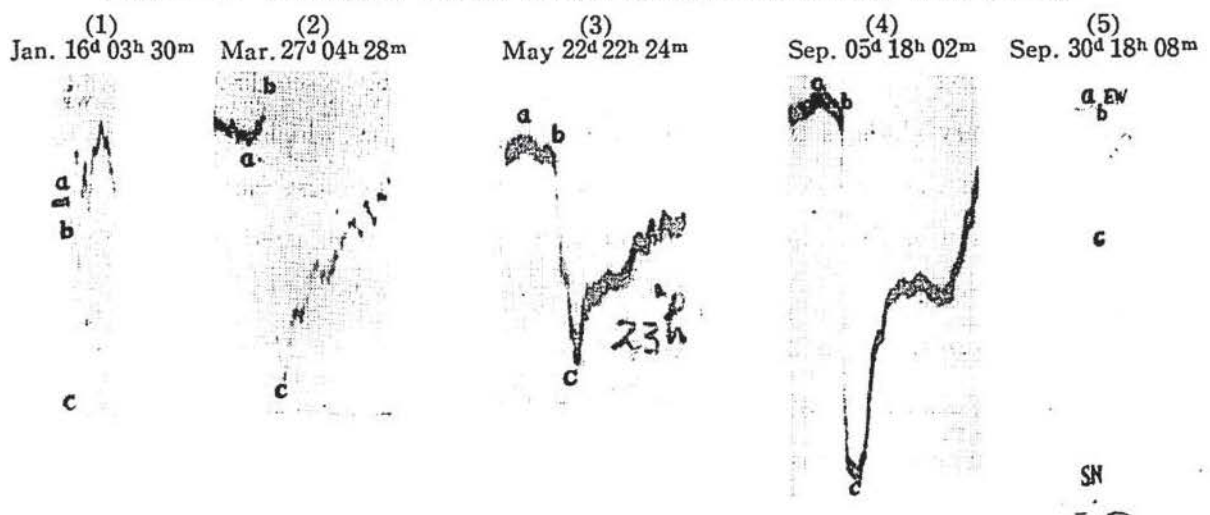


Fig. 74. Schematic figure of A-type and B-type of preliminary changes of *SSC* and *SI*.

kind of preliminary characteristic change was frequently followed by *SSC* or *SI* change. It was strange to us to see that even when they started on the very smooth electrograms free from any minor fluctuations, some *SSC*'s or *SI*'s were anticipated by small gradually increasing or decreasing preliminary changes lasting some minutes. Some typical

Plate 1~5. Preliminary changes for east-component at Kakioka, 1947. (U. T.)



Magnification factor : (1):1.0; (2):2.7; (3):2.7; (4):2.7; (5):0.8.

examples of these preliminary changes are shown in Plate (1)~(5), together with the exaggerated schematic expression in Fig. 74. In the figure the part a~b is meant by the present preliminary change of *SSC* or *SI*, and classified into A-type and B-type, respectively, according to its relative motion to the main first movement. As seen from the plate(5) the preliminary change is entirely distinguished from so-called a preliminary impulse or kick of *SSC** (arrow mark in *SN*), the latter being recorded almost as a segment of a line on the usual electrogram with revolving speed 1.5~2.0 cm per hour. Since the magnitude, A_p , and duration time, T_p , of the preliminary change approximately amount to a few percent of A_c and some minutes, respectively, the records were read out by means of a tenfold power micrometer. The preliminary changes adopted here are limited to all changes which have their duration times less than ten minutes and monotonously merge into the main impulses. When *SSC* or *SI* is occurred during disturbances, corresponding preliminary change is omitted. Of course, *SSC** with a preliminary inverse kick is included in A-type or B-type according to the criterion for the preliminary change.

In Table 33 are given the results of classification of the type of all available preliminary changes occurred in the sunspot maximum year, 1947, together with data of inverse kicks of sudden comments. The type is determined from the record at Kakioka, and ? marks indicate some preliminary changes not measurable correctly for some reasons, say, faint image of record, accidental coincidence with time marking, masking effect by disturbances and etc. The cross mark indicates that it is difficult to attribute any type to the variation considered.

Concerning the frequency of each type it is surprising to see that out of available thirty preliminary changes twenty three belong to the A-type, which is too many to be expectable from the view of a mere chance. This is the first fact that we should pay our attention to the immediate part of an electrogram anticipated to any *SSC* or *SI* change.

(B). Relation between T_p and T_c

The results of readings of T_p and T_c , duration time of the main in pulse, for east-component are given in Table 34. As seen in Fig. 75, there exists approximately a linear connection between T_p and T_c , and on the average $T_p \simeq T_c$. The relation seems to hold good for both A-and B-type. For purpose of reference it was checked

Table 33. Type of preliminary changes (P.C.) and distribution of inverse kicks of SSC and SI of earth-currents observed in Japan.

Date (U. T.)	Type of P. C.	Inverse Kick										Remark	
		Kakioka		Morioka		Haranomachi		Owashi		Miyakonojo			
Jan. 14 11 16	A			?	?								SSC
16 03 30	A			E	N								SSC
24 06 20	B			E?	N	E							SSC
24 23 51	A			—	?		—						SSC
Feb. 07 08 14	A			?	?								SI
16 03 00	A					—	—			—	—		SSC
Mar. 02 04 00	?							E	N	—	—		SI
02 18 17	A	E	N	E	N	E	N			—	—		SSC
07 05 36	B			E	N	E?		E		—	—		SI
12 04 56	A							—	—	—	—		SSC
27 04 28	B	N?	E?	E?	N	E	N			E	N		SSC
Apr. 02 10 15	A			—	—		N?			—	—		SI
03 15 02	?			E	N		N	E	N				SI
08 21 49	A	E	N	E?	N	E?	N					—	SSC
17 12 25	A	E	N?			E	N					N	SSC
May 15 00 18	?			—	—	—	—	—	—	—	—		SI
22 22 24	A						N			?			SI
23 02 40	B			E	?	—	—			—	—		SI
24 06 45	A	E	N		?			E	N	—	—		SSC
Jun. 05 07 27	A	E	N	E	N			E	N	—	—		SSC
13 17 49	X	E	N	E	N	E	N	E	N	—	—		SSC
17 03 00	?			—	—	E	N			—	—		SI
Jul. 17 10 37	A					E	N	—	—	—	—		SI
17 17 49	B						N	—	—	—	—		SSC
Aug. 15 09 51	A			—	—				N	E?			SSC
22 09 11	?			E	E				N				SSC
Sep. 02 23 26	A						N			—	—		SSC
04 13 45	A									—	—		SI
05 18 02	A				N					—	—		SSC
23 03 23	?									—	—		SSC
30 18 08	A		N		N					—	—		SSC
Nov. 09 08 56	A			—	—								SSC
11 06 51	B			—	—								SI
24 17 56	A		N						—		N		SI
27 18 35	B			—	—					—	—		SI
Dec. 01 08 53	A			—	—					—	—		SI
23 11 24	A							—	—	—	—		SI

Table 34. Values of amplitude and duration time of the main impulse and preliminary change at Kakioka for east-component. unit : minute and mV/km

Date (U. T.) 1947			T _p	T _c	A _p	A _c	A _p /A _c	
	d	h	m					
Jan.	04	11	16	2.0	2.8	10.4	107.8	0.096
	16	03	30	1.6	1.6	16.5	154.2	0.107
	24	06	20	1.2	1.6	6.4	55.1	0.116
	24	23	51	1.5	0.8	9.2	78.8	0.116
Feb.	07	08	14	1.3	1.6	6.5	63.1	0.103
	16	03	00	0.8	0.9	13.9	102.0	0.136
Mar.	02	04	00	?	?	?	?	?
	02	08	17	1.1	1.1	6.5	24.1	0.025
	07	05	36	0.2	0.4	9.2	91.5	0.101
	12	04	56	4.4	4.4	10.2	74.2	0.138
	27	04	28	2.4	3.0	9.2	103.0	0.089
Apr.	02	10	15	1.9	3.1	1.8	37.6	0.048
	03	15	02	?	?	?	?	?
	08	21	49	1.2	1.6	2.7	127.0	0.021
	17	12	25	2.1	1.9	5.4	279.6	0.020
May	15	00	18	?	?	?	?	?
	22	22	24	4.0	4.0	6.7	85.2	0.067
	23	02	40	1.1	1.1	16.3	102.3	0.159
	24	06	45	1.1	1.6	20.1	233.3	0.086
Jun.	05	07	27	0.8	0.8	4.8	329.2	0.015
	13	17	49	—	—	—	—	—
	17	03	00	?	?	?	?	?
	17	10	37	1.9	1.7	2.8	37.6	0.074
Jul.	17	17	49	0.8	1.0	18.7	413.2	0.045
	15	09	51	2.2	1.6	8.2	161.0	0.051
Aug.	22	09	11	?	?	?	?	?
	02	23	26	2.2	2.2	8.2	92.4	0.089
Sep.	04	13	45	3.6	2.8	10.4	93.3	0.110
	05	18	02	3.2	3.2	4.5	66.3	0.068
	23	03	23	?	?	?	?	?
	30	18	08	2.8	2.4	1.1	95.0	0.012
	09	08	56	3.4	4.0	4.3	65.5	0.065
Nov.	11	06	51	2.6	2.9	6.4	71.2	0.090
	24	17	56	3.2	2.8	2.2	79.0	0.045
	27	18	35	4.2	4.8	1.8	48.8	0.037
	01	08	53	2.5	2.7	3.7	81.2	0.045
Dec.	23	11	24	1.3	1.3	3.7	97.0	0.038

by the data of 1946 with regard to the A-type. These are the second fact to suggest something about the existence of some anticipated phenomena for the world-wide disturbances, SSC and SI.

[C]. Relation of A_p to A_c

The values of A_p and A_c for east-component at Kakioka are given in Table 34, and connection between them is graphically shown in Fig. 76.

Roughly speaking, there is a tendency that A_p increases with increasing A_c ,

although points in the figure are remarkably scattered. But the following two points are noticeable, (1) A_p 's of the A-type with kicks are very small as compared with others, making the lowest boundary line of the domain in which all observational points are contained; (2) Observational points seem to converge to a common point ($A_p=0, A_c \approx 15$ mV/km), in other words, at Kakioka A_c less than this value might not be accompanied with A_p , or such a small A_c might be forbidden to occur entirely. Concerning the item (2), the frequency spectrum with regard to the amplitude of SSC may be

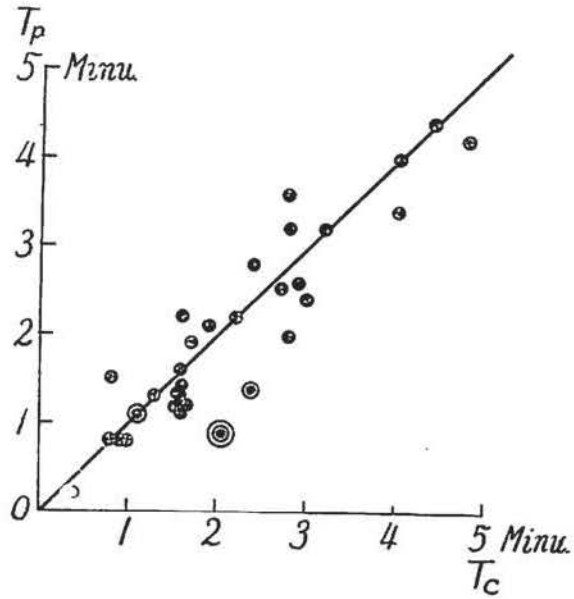


Fig. 75. Correlation between T_p and T_c of the preliminary change at Kakioka.

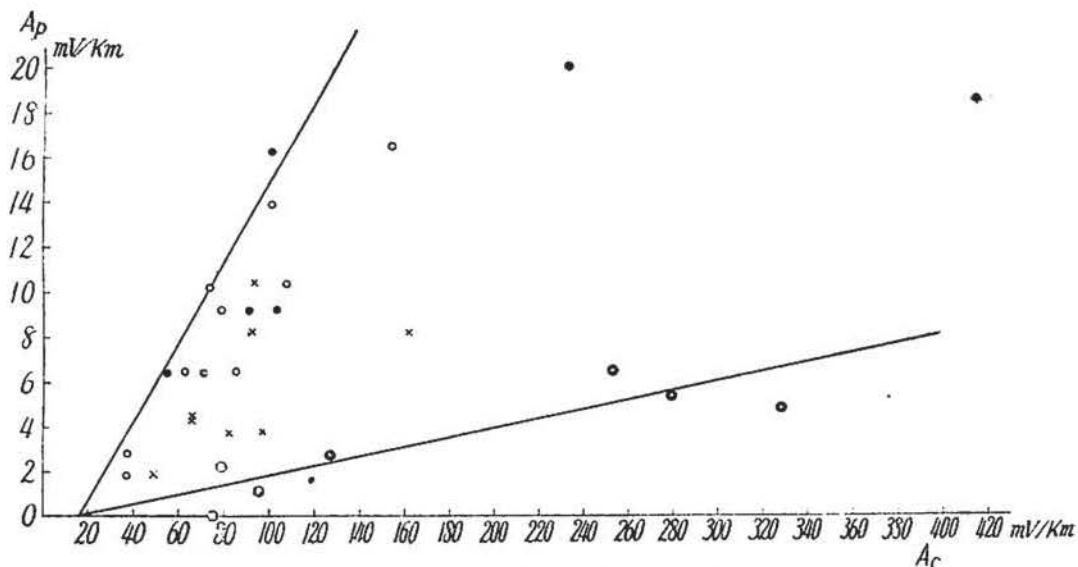


Fig. 76. Relationship between A_p and A_c of the preliminary change at Kakioka.

Table 35. Frequency spectrum of A_c for east-component at Kakioka, 1945~1949.

A_c (mV/km)	0~14	15~19	20~24	25~29	30~39	40~49	50~59	60~69	70~79
Numbers	1	5	6	8	19	17	15	13	16
A_c	80~89	90~99	100~109	110~119	120~129	130~139	140~149	150	
Numbers	7	17	11	5	5	3	1	17	

advisable, which is given in Table 35 for the interval of five years from 1945 to 1949 centering in 1947. From this table it is obvious that A_c contained in the interval 0~14 mv/km occurred only once out of one hundred and sixty six, and so as the lowest magnitude of A_c for east-component at Kakioka may be taken as the same value as that defined by a common point before-mentioned. Regarding (1), it is considered that A_p may be decreased due to superposition of an inverse change of kick. These facts are the third point to suggest some preliminary changes immediately before SSC and *SI*.

(D). *Diurnal and seasonal variation of A_p/A_c*

The amplitude ratio, A_p/A_c , is plotted in Fig. 77(A) with regard to the nearest hour of occurrence, where the material for the A-type in 1946 is supplied to get more numerous points for each hour. The average curve shows a predominant maximum and minimum around noon and 18 hr, respectively. And the difference between two three-hour means of A_p/A_c centering at these hours is statistically high significant. Although the observational points are less numerous during night hours, the curve seems to have a minor maximum and minimum before midnight and near 6 hr, respectively.

Concerning the daily variations of A_p and A_c themselves, they are shown separately in Fig. 77(B), in which the daily variation of A_p shows a fairly good agreement with that of A_p/A_c , but not so distinct for A_c as far as the present data are concerned. Therefore, the mode of the daily variation of A_p/A_c presented here is mainly responsible for that of A_p , though a minimum of A_p/A_c around 18 hr may be more exaggerated by some larger values of A_c appeared near the hour.

Any definite seasonal variation of A_p/A_c could not be obtained from the present

small material, and so is desirable a longer period statistics.

The solar daily variation of the amplitude of the preliminary change is the fourth fact to support the foregoing statement, considering a similar local time variation of that of sudden commencements.

3. *Diurnal variation of A_p and Sq -variation*

On the other hand it has been recently pointed out that so-called world-wide phenomena such as SSC, or SSC* of the geomagnetic field should not be left alone as they were, but re-examined taking such facts as their newly found local characteristics with regard

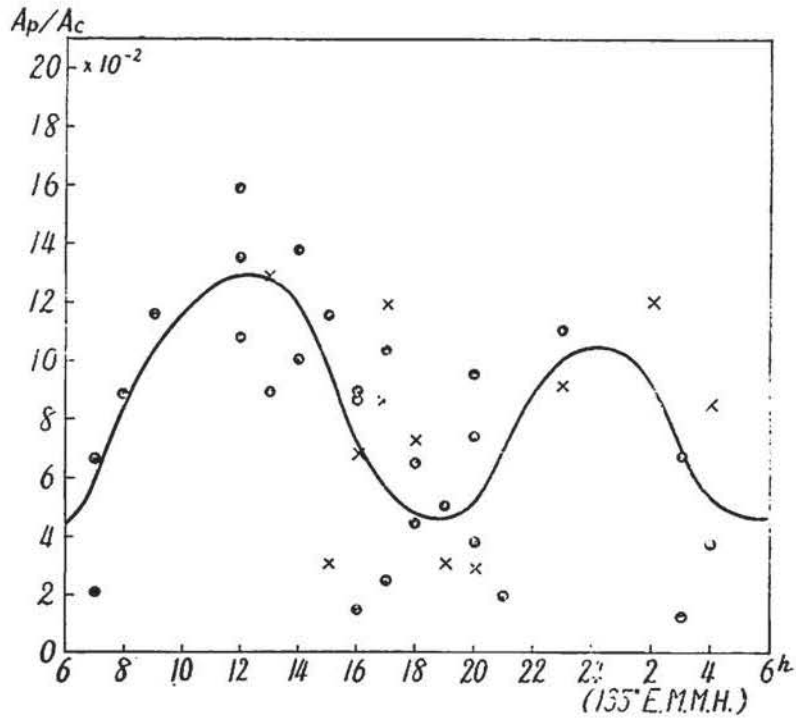


Fig. 77(A). Daily variation of A_p/A_c of the preliminary change at Kakioka.

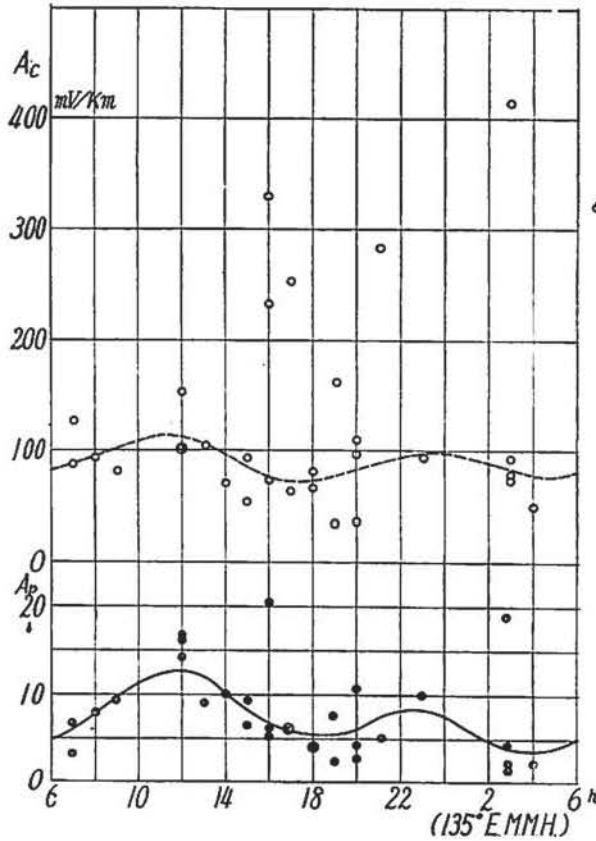


Fig. 77(B). Daily variations of A_p and A_c at Kakioka.

to the hourly frequency of occurrence as well as amplitude into consideration. The phenomena pictured up here may also introduce an another fact to be clarified from the same point of view. Here, the writer suggests that a part of the original current of SSC or SI may flow in our ionospheres.

If we compare the diurnal variation curve of A_p shown in Fig. 77 with that of S_q , we can easily find out a striking resemblance to each other except that the former lags about three hours behind the latter. So the correlation between A_p and each monthly mean S_q , of which phase angle is retarded three hours, is graphically shown in Fig. 78. A statistical test of significance of the linear correlation is made by the method of variance as shown in Table 36. The ratio of the variance (1) and (2) is 9.21. For 1 and 28 degrees of freedom the 5% and 1% values of F in the F -distribution are 4.20 and 7.64, respectively. It follows that the regression is significant, i. e. the tendency for large values of A_p to be associated with large values of the retarded S_q -variation is significant.

Table 36. Analysis of variance of regression.

Source of Variance	Sum of Squares	Degree of Freedom	Variance
(1) Due to Regression (C^2/S_x)	188.18	1	188.18
(2) About Regression ($S_y - C^2/S_x$)	571.70	28	20.42
Total	759.88	29	

$$S_x = \sum x^2 - (\sum x)^2/n, \quad S_y = \sum y^2 - (\sum y)^2/n, \quad C = \sum xy - \sum x \cdot \sum y/n,$$

$$x = S_q, \quad y = A_p - 7.7, \quad n = 30.$$

Some years ago this writer suggested to consider anew the solar daily variation field or some radiation agency for the interpretation of the local time variation of the hourly frequency of SSC or SSC.^{*(32)} Yet no plausible opinion has been brought forward up to date, meanwhile a local time variation of A_p with a striking resemblance to S_q -variation has been newly presented here. Now, it may be further

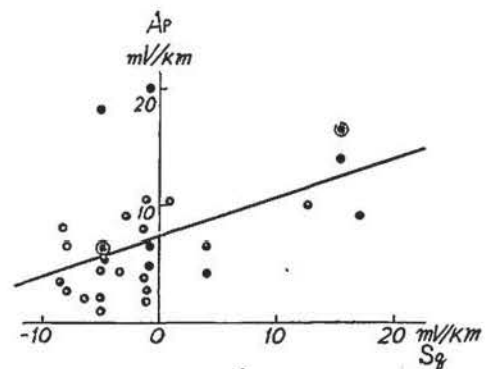


Fig. 78. Relationship between A_p and S_q for 1947.

suggested that at least a part of currents responsible for Ap, probably for SSC or SI, flow in or near the E-layer.

On the other hand it has been well known that the amplitude of SSC becomes larger with increasing latitude, and T. Nagata and his collaborators⁽⁸³⁾ have recently showed that Ds-field begins to appear in high latitudes from the very time of SSC, suggesting some corpuscular impinging upon the auroral zone ionospheres at the time. The origin of preliminary changes considered here may also be situated in high latitudes, and current distribution may take such a type as that of a polar storm. But the phenomena relies almost for its full account including an explanation of the phase angle mentioned above on the accumulated world-wide data in future.

4. *Preliminary inverse impulse, or kick of SSC* of earth-currents*

Regarding geomagnetic SSC*, among all investigators, T. Nagata⁽⁸⁴⁾ recently carried out the most comprehensive investigations, and so here something about the matter will be described from a standpoint of locality of earth-currents. From the data of 1947 at Kakioka four and nine SSC* for geomagnetic field and earth-currents can be respectively taken out, of which three SSC*'s occurred simultaneously in both fields. If geomagnetic SSC*'s corresponding to ? marks in Table 33 are counted in, the number increases to seven, of which five become to occur simultaneously with those of earth-currents. Therefore, it should be first admitted that all SSC's of earth-currents are not always accompanied simultaneously with geomagnetic ones; the former being more numerous. The second point to be mentioned is that SSC*'s of earth-currents are not always simultaneously observed at all five stations in Japan as given in Table 33.

Concerning these local characteristics of earth-currents, following two explanations may be possible. (a). All SSC*'s are supposed to be occurred simultaneously in both earth-currents and geomagnetic field, but small rapid ones are apt to appear in earth-currents only. This opinion assumes first that by using suitable technique so numerous kicks are to be observed even in the geomagnetic field in the lower latitudes, and a lack of simultaneity of earth-currents in a rather small area such as Japan is responsible for some inhomogeneity of electric structure of the ground, or such local

structure of the ionosphere over some specified region. (b). Even when there is no primary agency of SSC* in the geomagnetic field, there may be a good chance to observe SSC*-like kick of earth-currents in conjunction with the principal direction, provided some suitable direction and quickness of time change of the first starting vector of a geomagnetic SSC. These apparent SSC*'s may be superposed on primary ones.

For example, the direction of the first starting magnetic vector in Japan is generally north-easterly⁽⁸⁶⁾ and may change in some range of degrees. So at a station with the south-westerly principal direction will be more numerous such lucky chances for north-component than east-component (Table 33).

Unfortunately, there are few key points to decide which opinion is more plausible. The writer, however, is now inclined to consider the case (b) more promisingly than (a), although the latter would be more interesting from a geophysical point of view. At any rate, carefully conducted simultaneous quick-run recordings of both geomagnetic elements and earth-currents will answer this question, especially provided high sensitive instruments and accurate timekeeping.

In conclusion it may be worthy to add some words about a question whether or not some other variations do manifest such changes as preliminary changes before-mentioned or kicks. Some well-known variations such as pulsations, solar flare variations, bays and etc. are unlikely to show such characteristic changes, but further efforts should be offered to examine for other rapid changes frequently observed during storms.

Conclusions for the Chapter II

1. It was endeavoured to collect recent data as many as possible from various parts of the world together with our Japanese observations, and to analyse them to deduce some general pictures of local characteristics as well as world-wide natures of the spatial distribution and time variations of earth-currents.

2. First of all the principal direction, or restricted direction of earth-currents, was examined by using the hodographs of the annual mean Sq observed at several stations in U. S. A., Europe, South-America, Japan, Australia and so on, as well as short period variations recorded at about two dozens of stations in Japan. In spite of

apparently random distribution of the direction, we may finally deduce three groups of type, correlating to the actual distribution of land and sea, and topographical and geological circumstances together with earth-resistivity surveys around the stations. At several stations the direction is almost constant even for each individual harmonic wave of Sq, and if except for the diurnal waves at some stations, twelve stations out of seventeen ones belong to this catalogue. So there are few stations at which principal directions deduced separately from each harmonic wave are not always equal, but somewhat different one another; for example, at Kakioka both diurnal and semidiurnal harmonics in winter are responsible for this inequality.

3. Comparing the year-to-year change of the maximum range of the Sq-variation of earth-currents to that of relative sunspot numbers, we obtained a nearly linear correlation between them, of which proportional constant to S approximately depends neither upon the base direction nor coordinates of latitude of stations. The east-component at Kakioka, however, was found to be exceptionally small compared with an expectable value from the linear expression said above, and to be attributed to the winter characteristics of the mode of Sq. Of course, a similar consistent result can be obtained for each harmonic wave of Sq. The facts lead us to study how does the mode of Sq change in the long course of years at any station situated near the locus of the wandering focus of the equivalent current system of the Sq field.

4. There is found a remarkable long period variation of $T_{\min}^{\#}$ of Sq, time of occurrence of the extreme minimum for east-component in winter at Kakioka, which has a distinct maximum about two years before the maximum of S and shows a good parallelism with the change of $\Delta S/\Delta t$, not S itself, where S is the relative sunspot number and t time in unit of year. We have no such a change for $T_{\max}^{\#}$, time of occurrence of the extreme maximum for east-component of Sq in winter. There is also found a similar variation in the geomagnetic Sq field, especially in the horizontal intensity at Kakioka, and a tendency of less significance at Tucson, an another similar middle latitude station.

5. An another interesting aspect of the secular variation of the mode of Sq in winter at Kakioka is that there exists some shorter period, namely, four-year period variation superposed on the long period change before-mentioned. We can detect similar periodic variations in both geomagnetic Sq at Kakioka and $f_{P_2}^{\circ}$ at Kokubunji,

Tokyo, as well as relative sunspot numbers S .

6. On the other hand, phase angles φ_n 's of harmonic waves of Sq show no systematic connection with S as a whole, contrary to the amplitude changes, though φ_1 manifests apparently random large fluctuations, especially in north-component. However, the year-to-year change of φ_n is fairly systematic for each wave, but there is a remarkable dissimilarity between φ_1 and other φ 's, namely, the former manifests the long period change before-mentioned, while the latter 4-year period changes. These two characteristics correspond to those of $T_{\text{min.}}^E$, namely, n or N and Δn , respectively, showing distinct different contributions from different harmonic waves to an apparent secular change of the mode of Sq at Kakioka. At Tucson, however, there is found no such 4-year period changes for φ_n 's, while φ_1 's at both stations show the similar long period change. This discrepancy may be responsible for the different behaviors of the ionospheres in winter over the stations. Further investigations will be desirable from both sides of the geo-electromagnetic field and ionosphere by gathering longer period data from various places in the world.

7. Concerning the solar daily variations observed at seventeen stations, the magnitude of the resultant potential gradient $R_{n,o} = \sqrt{C_{n,o}^N{}^2 + C_{n,o}^E{}^2}$ is of order of some millivolts per kilometer at most, except for two stations, Toledo and Nemuro with exceptionally small and large values, respectively. The average values for twelve middle latitude stations are as follows.

Period (hrs)	24	12	8	6
Amplitude (mV/km)	1.51	1.86	1.22	0.43

8. It is confirmed that the ratio of $R_{n,o}$ to $H_{n,o} = \sqrt{C_{n,o}^X{}^2 + C_{n,o}^Y{}^2}$ is approximately proportional to $1/\sqrt{T_n}$ even in many different localities in the world as far as such a range of T_n that covers those of principal harmonics of the Sq-variation is concerned. This relationship, however, deviates from its lineality with increasing $1/\sqrt{T_n}$; for example, at all four station in Japan the specific resistance of the ground increases with increasing depth from the surface. Assuming a proper uniform specific resistance of the upper several kilometers depth, a presumed two-layer structure of the ground fits fairly well to each station.

9. Apparent resistivities ρ_a 's calculated from $R_{n,o}/H_{n,o} = \sqrt{\rho_a/2T_n}$ are of order of $10^4 \Omega \cdot \text{cm}$ at nine stations out of fifteen, while they are as small as $3 \sim 4 \cdot 10^3 \Omega \cdot \text{cm}$

at Huancayo and Toledo. The average value of ρ_a 's for twelve middle latitude stations gives $4 \cdot 10^4 \Omega \cdot \text{cm}$.

10. There is a fairly intimate connection between ρ_a 's and earth-resistivities ρ_{obs} 's, which are observed in the shallow upper portion of the earth up to some hundred meters or more below the surface, as far as the present observed earth-resistivities are concerned.

11. The second harmonic wave of S_q near the sea-coast contains a factor of which amplitude decreases towards the inner part of the land with increasing distance measured from the nearest sea-coast to the respective stations. Since it is examined in vain to get such a regular distribution for the other waves, it is suggested that some local earth-currents due to, say, electrochemical actions or capillary fluid motions may be produced near the sea-coast by the solar tidal motion of the sea-water.

12. It is pointed out that *SSC* and *SI* changes are generally anticipated by small gradually increasing or decreasing preliminary changes lasting some minutes. These preliminary changes are characterized by four observational facts which suggest us to pay our attentions to the immediate parts of the electrogram anticipated to *SSC* and *SI* changes. The four observational characteristics of the preliminary change are as follows, (1) Preponderance of the frequency of one specified type of the variation, *A*-type; (2) Duration time of the variation, T_P , is almost equal to that of the main impulse, T_C ; (3) Amplitude of the preliminary change, A_P , is distributed within a definite domain of the (A_P, A_C) diagram; (4) The solar daily variation of the amplitude of the preliminary change.

13. The solar daily variation of A_P shows a striking resemblance with S_q -variation, though the phase angle of the former lags about three hours behind the latter. This suggests that at least a part of currents responsible for A_P , probably *SSC* or *SI*, may flow in or near the E-Layer.

14. All *SSC*'s of earth-currents are not always accompanied simultaneously with geomagnetic ones, the former being more numerous. *SSC*'s of earth-currents are not always simultaneously observed at all five stations in Japan. These local characteristics of earth-currents may be considered to be mainly controlled by suitable combinations of the direction and quickness of the first impulse change with the electric structure of the ground around the very station.

References

- (26) Terr. Magn. **36**, No. 2 (1931), 1907.
- (27) Terr. Magn. **33**, (1928), 205~209.
- (28) Terr. Magn. **32**, (1927), 143~145.
- (29) Terr. Magn. & Elect., Chapter VI Earth-Currents (1949).
- (30) Ency. Britanica, Vol. VIII, 815 (8th Ed.)
- (31) Jour. Met. Soc. Jap. **12**, No. 1; Ann. Rep. of Toyohara Mag. Obs.
- (32) Ann. Rep. of Kakioka Mag. Obs.
- (33) Terr. Magn. **40**, No. 3 (1935), 317~324.
- (34) Corrientes Teluricas Año 1948, Observatorio Central Geofisico de Toledo.
- (35) K. Maeda, 地震 (Earthquake), **9**, No. 7 (1937).
- (36) T. Nagata, 地震 (Earthquake) **15**, No. 11 (1943).
- (37) Y. Yokouchi, Memo. Kakioka Mag. Obs., **5**, No. 1 (1943).
- (38) Y. Kato, Jap. Jour. Astr. & Geophy., **1**, No. 4 (1943).
- (39) Yamakawa Ionospheric Obs.
- (40) K. Hirao, Geophy. Notes, Tokyo Univ., No. 29 (1947).
- (41) K. Hirao, Special Committee for the study of the Fukui Earthquake (1950), 181.
- (42) Terr. Magn. **40**, No. 3 (1935), 237~254.
- (43) Terr. Magn. **32**, No. 1, 49~63.
- (44) Terr. Magn. **27**, 1~30 (1922).
- (45) Ann. Rep. of Toyohara Mag. Obs., 1933~1936.
- (46) 理科年表 (Rika Nenpyo), 1955.
- (47) M. Hasegawa and M. Ota, Read before the meeting of the Section of Terr. Mag. and Elect., N.P.C. Japan (Feb. 1941).
M. Ota, Rep. of Ionosphere Res. Japan, **3**, No. 1~2 (1949).
T. Nagata, Geophy. Notes, Tokyo Univ., No. 36 (Feb. 1948).
- (48) (47)
- (49) (1)
- (50) Terr. Magn. **50**, No. 3 (1945), 175~184.
- (51) (46)
- (52) (46)
- (53) (1)
- (54) Boletín Mensual Vol. 6~7 (1951~1952), Observatorio De Física Cosmica De San Miguel (R. Argentina).
- (55) Canadian Polar Year Expeditions, 1932~1933, Vol. II.
- (56) Geomagnetismo Año 1949, Obs. Cent. Geof. de Toledo.
- (57) L. A. Bauer, Terr. Magn, **27** (1922), 1~30.
- (58) Year Books for Tucson (Ariz.), 1919~1920, U.S. Coast and Geodetic Survey.
- (59) Ann. Rep. Toyohara Mag. Obs.
- (60) Ann. Rep. Kakioka Mag. Obs.

- (61) Res. Dep. Terr. Magn. Vol. VII-A, Carnegie Inst., Washington.
- (62) Res. Dep. Terr. Magn. Vol. X-A, Carnegie Inst., Washington.
- (63) L. Cagniard, Geophysics Vol. XVIII, No. 3 (1953), 605~635.
T. Rikitake, Bull. Earthq. Res. Inst. Tokyo Univ., Vol. XXIX (1951).
- (64) Corrientes Teluricas Año 1949, Obs. Cent. Geof. de Toledo.
- (65) Terr. Magn. **32**, No. 1 (1927), 49~63, ; **33** (1928), 79~90.
- (66) Terr. Magn. **39**, No. 3 (1934), 199.
- (67) Terr. Magn. **35**, No. 2 (1930), 61~72).
- (68) (65)
- (69) M. Hirayama, Jour. Met. Soc. Jap. **12**, No. 1 (1934), 16~22.
- (70) S. Omote, Bull. Earthq. Res. Inst. Tokyo Univ., Vol. XXIX, Part I (1951).
- (71) Terr. Magn. **43**, No. 2 (1938), 107~118.
- (72) J. Egedal, Terr. Magn, **42** (1937), 179~181.
- (73) Y. Yokouchi, Memo. Kakioka Mag. Obs. **2**, No. 2, 3 (1939), 65~18.
- (74) M. Hasegawa, Rep. Jap. Ass. Adv. Sci., **14**, No. 2 (1942).
- (75) Y. Yokouchi, Read before the 16th general meeting of Soc. Terr. Magn. & Elect. Japan (1954).
- (76) S. Ogura, 潮汐 (Ocean Tide).
- (77) (76)
- (78) Z. Yasukura, Tech. Rep. Kyushu Univ., (1934), 1~11.
- (79) (76)
- (80) T. Terada, Bull. Earthq Res. Inst. Tokyo Univ., Suppl. I (1934), 25~34.
- (81) T. Yoshimatsu, Journ. Geomag. Geoelec., II No. 2 (1950), 54~60.
- (82) (81)
- (83) For example, T. Nagata and N. Fukushima, Indian J. Met. Geophys., **5**, Special. geomagnetic number (1954), 75~88.
- (84) T. Nagata, Rep. Ionosphere Res. Japan, VI, No. 1 (1952), 13~30.
- (85) Y. Yokouchi, Memo. Kakioka Mag. Obs. **6**, No. 2 (1953), 204~248.
T. Yumura, Memo. Kakioka Mag. Obs. **7**, No. 1 (1954), 27~48.